Article

Coenzyme Q headgroup intermediates can ameliorate a mitochondrial encephalopathy

https://doi.org/10.1038/s41586-025-09246-x

Received: 30 April 2024

Accepted: 5 June 2025

Check for updates

Guangbin Shi[1,2,11], Claire Miller[3,11], Sota Kuno[1,2], Alejandro G. Rey Hipolito[4], Salsabiel El Nagar[5], Giulietta M. Riboldi[3], Megan Korn[2,6], Wyatt C. Tran[2,6], Zixuan Wang[1,2], Lia Ficaro[7], Tao Lin[4], Quentin Spillier[1,2], Begoña Gamallo-Lana[8], Drew R. Jones[1,6,7], Matija Snuderl[9], Soomin C. Song[10], Adam C. Mar[8], Alexandra L. Joyner[5], Roy V. Sillitoe[4], Robert S. Banh[2,6] & Michael E. Pacold[1,2] ✉

Decreased brain levels of coenzyme Q_{10} (CoQ_{10}), an endogenously synthesized lipophilic antioxidant[1,2], underpin encephalopathy in primary CoQ_{10} deficiencies[3,4] and are associated with common neurodegenerative diseases and the ageing process[5,6]. CoQ_{10} supplementation does not increase CoQ_{10} pools in the brain or in other tissues. The recent discovery of the mammalian CoQ_{10} headgroup synthesis pathway, in which 4-hydroxyphenylpyruvate dioxygenase-like protein (HPDL) makes 4-hydroxymandelate (4-HMA) to synthesize the CoQ_{10} headgroup precursor 4-hydroxybenzoate (4-HB)[7], offers an opportunity to pharmacologically restore CoQ_{10} synthesis and mechanistically treat CoQ_{10} deficiencies. To test whether 4-HMA or 4-HB supplementation promoted CoQ_{10} headgroup synthesis in vivo, here we administered 4-HMA and 4-HB to *Hpdl*$^{-/-}$ mice, which model an ultra-rare, lethal mitochondrial encephalopathy in humans. Both 4-HMA and 4-HB are incorporated into CoQ_9 and CoQ_{10} in the brains of *Hpdl*$^{-/-}$ mice. Oral treatment of *Hpdl*$^{-/-}$ pups with 4-HMA or 4-HB enables 90–100% of *Hpdl*$^{-/-}$ mice to live to adulthood. Furthermore, 4-HB treatment stabilizes and improves the neurological symptoms of a patient with progressive spasticity due to biallelic *HPDL* variants. Our work shows that 4-HMA and 4-HB can modify the course of mitochondrial encephalopathy driven by *HPDL* variants and demonstrates that CoQ_{10} headgroup intermediates can restore CoQ_{10} synthesis in vivo.

Many common diseases are associated with decreased tissue CoQ_{10} levels[8]. Furthermore, some pharmaceuticals, such as statins, reduce CoQ_{10} levels, resulting in statin-associated muscle symptoms[9]. The perceived role of decreased tissue CoQ_{10} in diseases has fuelled a long-standing desire to replete tissue CoQ_{10} pools[10]. However, CoQ_{10} pools are refractory to pharmacological augmentation[11–13], particularly in the central nervous system, owing to the poor bioavailability[11,14] of CoQ_{10}. New therapeutic approaches are needed to address the limitations of CoQ_{10} supplementation or to promote endogenous CoQ_{10} synthesis.

A potential avenue of enabling CoQ_{10} synthesis in vivo is our recent discovery of the mammalian CoQ_{10} headgroup synthesis pathway[7], in which HPDL catalyses the synthesis of 4-HMA, which generates 4-HB, the immediate precursor of the CoQ_{10} headgroup[5,6,15] (Fig. 1a). Both 4-HMA and 4-HB are small molecules (<200 Da) that are readily taken up by cells and are efficiently incorporated into CoQ_{10}. Our work, and recent research showing that high doses of 4-HB rescue the survival of mice with hypomorphic *Coq2* (*Coq2*^{A252V})[16], indicates that 4-HMA and 4-HB might enable mammalian CoQ_{10} synthesis in patients with deficits in the CoQ_{10} headgroup synthesis pathway, providing a therapeutic strategy for patients with CoQ_{10} deficiencies.

To investigate this hypothesis, we tested whether 4-HMA and 4-HB could be used to treat *Hpdl*$^{-/-}$ mice, which robustly model neurodevelopmental disorder with progressive spasticity and brain white matter abnormalities (NEDSWMA)[17–23], an ultra-rare lethal primary CoQ_{10} deficiency caused by *HPDL* variants that presents with severe neurodevelopmental symptoms. *Hpdl*$^{-/-}$ mice develop movements consistent with spastic paresis and epileptic seizures and die by postnatal day 15 (P15)[21]. Here we show that treatment with 4-HMA or 4-HB restores CoQ biosynthesis in the brains of *Hpdl*$^{-/-}$ mice and demonstrate rescue of *Hpdl*$^{-/-}$ mice by supplementation with CoQ_{10} headgroup intermediates. We also show that 4-HB treatment improves neurological symptoms and modifies the clinical course of a patient with *HPDL* variants. Restoration of brain CoQ_{10} synthesis with CoQ_{10} headgroup intermediates might alleviate the neurological symptoms of primary CoQ_{10} deficiencies and diseases associated with low tissue CoQ_{10} pools.

[1]Department of Radiation Oncology, NYU Grossman School of Medicine, New York, NY, USA. [2]Laura and Isaac Perlmutter Cancer Center, NYU Langone Health, New York, NY, USA. [3]Department of Neurology, The Marlene and Paolo Fresco Institute for Parkinsons and Movement Disorders, NYU Grossman School of Medicine, New York, NY, USA. [4]Department of Pathology and Immunology, Baylor College of Medicine, Jan and Dan Duncan Neurological Research Institute, Texas Children's Hospital, Houston, TX, USA. [5]Developmental Biology Program, Sloan Kettering Institute, Memorial Sloan Kettering Cancer Center, New York, NY, USA. [6]Department of Biochemistry, NYU Grossman School of Medicine, New York, NY, USA. [7]Metabolomics Core Research Laboratory, NYU Grossman School of Medicine, New York, NY, USA. [8]Department of Neuroscience and Physiology Neuroscience Institute, NYU Grossman School of Medicine, New York, NY, USA. [9]Department of Pathology, NYU Grossman School of Medicine, New York, NY, USA. [10]IonLab, Department of Pathology, NYU Langone Health, New York, NY, USA. [11]These authors contributed equally: Guangbin Shi, Claire Miller. ✉e-mail: michael.pacold@nyulangone.org

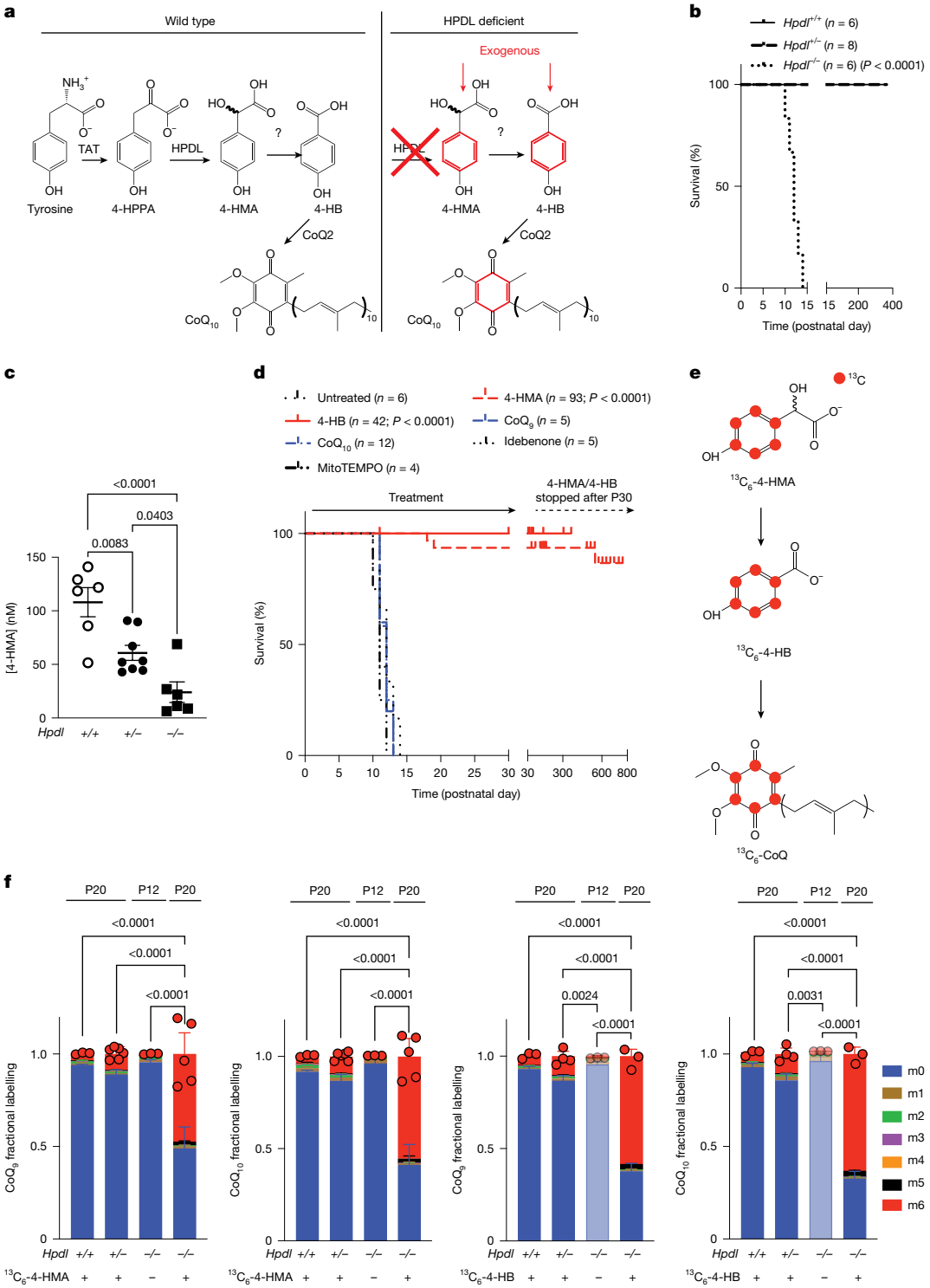


Fig. 1 | CoQ headgroup intermediates improve *Hpdl*$^{-/-}$ mouse survival and are incorporated into brain CoQ_9. **a**, The mammalian CoQ headgroup synthesis pathway. Left, tyrosine is deaminated to 4-hydroxyphenylpyruvate (4-HPPA). HPDL converts 4-HPPA to 4-HMA, which generates 4-HB. Right, supplementation of 4-HMA or 4-HB compensates for loss of HPDL activity. The carbon atoms from 4-HMA or 4-HB that enter the CoQ headgroup are highlighted in red. **b**, *Hpdl*$^{-/-}$ pups die by P15. *Hpdl*$^{+/+}$ and *Hpdl*$^{+/-}$ pups survive for more than one year. **c**, *Hpdl*$^{-/-}$ pups ($n = 6$) have lower plasma 4-HMA than *Hpdl*$^{+/+}$ ($n = 6$) or *Hpdl*$^{+/-}$ ($n = 8$) pups on P10. Data are mean ± s.d. **d**, Oral supplementation of 4-HMA and 4-HB (10 mg kg^{-1} per day) improves the overall survival of *Hpdl*$^{-/-}$ pups. CoQ_9, CoQ_{10} and related compounds do not improve *Hpdl*$^{-/-}$ pup survival. Treatment with 4-HMA and 4-HB was carried out until P30. 4-HMA-treated pups began treatment on P3–P5 except for three that began on P6 and one that began on P7. 4-HB-treated pups began treatment on P3–P5. **e**, Schematic of ^{13}C incorporation from $^{13}C_6$-4-HMA and $^{13}C_6$-4-HB into CoQ_9, increasing the mass of CoQ_9 by 6 Da (m6). **f**, Fractional labelling of brain CoQ_9 in mice fed $^{13}C_6$-4-HMA and $^{13}C_6$-4-HB (10 mg kg^{-1} once daily) from P3 to P20. Both $^{13}C_6$-4-HMA and $^{13}C_6$-4-HB are incorporated into $^{13}C_6$-CoQ_9 (m6) in *Hpdl*$^{-/-}$ mice. Data are mean ± s.d. $^{13}C_6$-4-HMA: *Hpdl*$^{+/+}$ $n = 3$, *Hpdl*$^{+/-}$ $n = 6$ and *Hpdl*$^{-/-}$ treated $n = 5$. $^{13}C_6$-4-HB: *Hpdl*$^{+/+}$ $n = 3$, *Hpdl*$^{+/-}$ $n = 4$ and *Hpdl*$^{-/-}$ treated $n = 3$. *Hpdl*$^{-/-}$ untreated $n = 3$. CoQ_9 and CoQ_{10} data from *Hpdl*$^{-/-}$ untreated mice were obtained in the 4-HMA experiment and are presented in a faded shade of colour in the 4-HB experiment for ease of interpretation Significance was tested by two-way analysis of variance (ANOVA) followed by Tukey's post hoc test. *P* values < 0.05 are presented on each plot. Survival data were analysed with the log-rank test.

4-HMA and 4-HB can treat *Hpdl*$^{-/-}$ pups

As previously described[21], *Hpdl*$^{-/-}$ pups do not gain weight as quickly as do *Hpdl*$^{+/+}$ pups after birth, develop seizures (Extended Data Fig. 1a,b and Supplementary Video 1) and die by P15 (Fig. 1b). *Hpdl*$^{-/-}$ pups have lower plasma 4-HMA concentrations than do *Hpdl*$^{+/+}$ or *Hpdl*$^{+/-}$ pups (Fig. 1c) and a higher plasma lactate:pyruvate ratio (Extended Data Fig. 1c).

We hypothesized that treatment of *Hpdl*$^{-/-}$ pups with the CoQ_{10} headgroup intermediates 4-HMA or 4-HB would improve the neurological symptoms of *Hpdl*$^{-/-}$ mice. 4-HMA and 4-HB are orally bioavailable with half-lives of 2.8 h and 0.35 h, respectively (Extended Data Fig. 1d and Supplementary Table 1) and neither compound induces inflammation or necrosis in the brain, heart, lungs, liver, kidneys or spleen of mice at single doses of 500 mg kg^{-1} or at a dose of 500 mg kg^{-1} per day for 3 months (Extended Data Fig. 1e). 4-HMA was detected in the plasma of 4-HMA-treated *Hpdl*$^{-/-}$ pups on P10 (Extended Data Fig. 1f).

Hpdl$^{-/-}$ pups treated orally with 4-HMA or 4-HB at a minimum of 10 mg kg^{-1} once daily starting on P3 or P7 gained weight and had improved mobility (Extended Data Fig. 1a,g, Supplementary Table 2 and Supplementary Video 2). *Hpdl*$^{-/-}$ pups treated on P10 did not survive (Extended Data Fig. 1h). After weaning, we treated *Hpdl*$^{-/-}$ pups with 10 mg kg^{-1} 4-HMA or 4-HB per day in their drinking water and discontinued 4-HMA or 4-HB treatment on P30. Most *Hpdl*$^{-/-}$ pups treated with 4-HMA or 4-HB lived for 18 months or more (Fig. 1d). By contrast, *Hpdl*$^{-/-}$ pups treated orally with CoQ_9, CoQ_{10}, the CoQ analogue idebenone or the mitochondrially targeted antioxidant MitoTEMPO[24–26] did not survive (Fig. 1d). We conclude that 4-HMA or 4-HB treatment extends the lifespan of *Hpdl*$^{-/-}$ pups to the average lifespan of a mouse.

4-HMA and 4-HB restore CoQ synthesis

To test whether 4-HMA and 4-HB crossed the blood–brain barrier and were incorporated into CoQ_9, the predominant coenzyme Q species in mice, and CoQ_{10}, which is also found in mouse brain, we treated *Hpdl*$^{+/+}$, *Hpdl*$^{+/-}$ and *Hpdl*$^{-/-}$ pups with $^{13}C_6$-4-HMA and $^{13}C_6$-4-HB, in which the ring carbons are labelled with ^{13}C, at 10 mg kg^{-1} per day from P3 to P20. We hypothesized that incorporation of all ring carbons from $^{13}C_6$-4-HMA and $^{13}C_6$-4-HB into CoQ_9 would result in $^{13}C_6$-CoQ_9 and $^{13}C_6$-CoQ_{10} (m6-CoQ_9 and m6-CoQ_{10}, respectively; Fig. 1e). In *Hpdl*$^{-/-}$ pups, at least 50% of CoQ_9 and CoQ_{10} came from $^{13}C_6$-4-HMA and $^{13}C_6$-4-HB (Fig. 1f). Treatment with $^{13}C_6$-4-HMA and $^{13}C_6$-4-HB also increased brain CoQ_9 and CoQ_{10} pools in *Hpdl*$^{-/-}$ pups (Extended Data Fig. 2a), albeit to levels lower than those of *Hpdl*$^{+/+}$ and *Hpdl*$^{+/-}$ mice[27], and these lower CoQ levels persisted after 4-HMA treatment was stopped (Extended Data Fig. 2b). 4-HMA did not increase CoQ_9 and CoQ_{10} levels in the brains of P90 wild-type mice (Extended Data Fig. 2c). These data show that *Hpdl* loss results in a primary CoQ deficiency in the brains of mice and that orally administered $^{13}C_6$-4-HMA and $^{13}C_6$-4-HB enable CoQ_9 and CoQ_{10} synthesis in the brain.

4-HMA improves histology of *Hpdl*$^{-/-}$ pup brains

CoQ_{10} is essential for electron transport chain activity and maintenance of the mitochondrial membrane potential[28]. *Coq8a*$^{-/-}$ mice develop cerebellar ataxia and have abnormal cerebellar mitochondrial morphology[29]. Moreover, primary CoQ_{10} deficiencies are a cause of cerebellar ataxia in patients[30]. Therefore, we examined cerebellar mitochondrial morphology and cerebellar morphology in *Hpdl*$^{-/-}$ pups. Electron microscopy revealed that mitochondria in the cerebella of P11 *Hpdl*$^{-/-}$ pups were smaller than those of *Hpdl*$^{+/+}$ or *Hpdl*$^{+/-}$ control pups and that mitochondria in the cerebella of *Hpdl*$^{+/-}$ pups were smaller than those of *Hpdl*$^{+/+}$ controls (Fig. 2a,b). 4-HMA increased cerebellar mitochondrial size in P11 *Hpdl*$^{-/-}$ pups, although not to the same size as those of *Hpdl*$^{+/+}$ pups (Fig. 2a,b). P11 *Hpdl*$^{-/-}$ pups had small cerebella, with a thinner external granular layer, vacuolization and intracellular oedema in cerebellar Purkinje cells (PCs) and depletion of the internal granular layer (Fig. 2c). Cerebellum size in *Hpdl*$^{-/-}$ pups was greatly reduced on P6 (Extended Data Fig. 3a–c), when these animals responded to 4-HMA (Extended Data Fig. 1h). Cerebellar histology in P6 and P11 *Hpdl*$^{-/-}$ pups and in P56–P57 mice was restored by 4-HMA supplementation (Fig. 2c and Extended Data Fig. 3a,h). Immunohistochemical staining for calbindin showed underdeveloped PC dendritic arbors in *Hpdl*$^{-/-}$ pups on P11 (Extended Data Fig. 3e,f). 4-HMA treatment largely restored PC dendritic arborization (Extended Data Fig. 3e,f and Extended Data Fig. 4a). Granule cell precursors in P11 *Hpdl*$^{-/-}$ pups had lower Ki-67 staining than did those in *Hpdl*$^{+/+}$ pups (Extended Data Fig. 3e,g). Ki-67 staining was restored by 4-HMA treatment (Extended Data Fig. 3e). Similarly, the external granular layer thickness was reduced in *Hpdl*$^{-/-}$ pups on P11 compared with *Hpdl*$^{+/+}$ and *Hpdl*$^{+/-}$ pups and was partially restored with 4-HMA treatment (Extended Data Fig. 3e,g). To determine whether these changes were initiated before P11, we analysed cerebellar morphology on P6. PAX6 staining revealed that granule cells were depleted in the external and internal granular layers of P6 *Hpdl*$^{-/-}$ pups relative to *Hpdl*$^{+/+}$ pups and was improved with 4-HMA treatment (Extended Data Fig. 3b). Calbindin staining of the PCs in P6 *Hpdl*$^{-/-}$ pups revealed a multilayer without dendrites. 4-HMA treatment resulted in a single layer of PCs with stunted dendrites (Extended Data Fig. 3b). The cerebella of P6 *Hpdl*$^{-/-}$ pups had higher TUNEL staining indicating cell death, which decreased with 4-HMA treatment of *Hpdl*$^{-/-}$ pups (Extended Data Fig. 3b,d). 4-HMA increased cerebellar size in P6 *Hpdl*$^{-/-}$ pups (Extended Data Fig. 3a,c).

The cerebral cortex of P11 *Hpdl*$^{-/-}$ pups showed no major changes in mitochondrial morphology (Extended Data Fig. 4b) but subtle loss of healthy cortical architecture (Extended Data Fig. 4c). The hippocampus was largely unremarkable (Extended Data Fig. 4d). However, TUNEL staining was higher in the cortex, striatum and thalamus of P6 *Hpdl*$^{-/-}$ pups and treatment with 4-HMA significantly decreased TUNEL staining in the striatum (Extended Data Fig. 5a).

These findings indicate that part of the phenotype of *Hpdl*$^{-/-}$ mice involves cell death associated with a delay in cerebellar maturation and increased cell death in the cortex, striatum and thalamus. Interestingly, metabolite-replacement therapy with 4-HMA, the metabolic product of HPDL, largely reverted these abnormalities. Our data demonstrate that 4-HMA-dependent CoQ synthesis is important for brain development and indicate that treatment with 4-HMA or 4-HB during infancy or childhood could improve the outcomes of patients with *HPDL* variants.

4-HMA improves *Hpdl*$^{-/-}$ PC function

To test whether *Hpdl* loss affected mitochondrial electron transport chain activity, we measured electron flow through complexes I, II and IV (Extended Data Fig. 6a) in mitochondria isolated from the brains of P9 *Hpdl*$^{+/+}$, *Hpdl*$^{+/-}$ and *Hpdl*$^{-/-}$ pups and P9 *Hpdl*$^{-/-}$ pups treated with 4-HMA. Consistent with loss of CoQ, electron flow through complexes I and II was reduced in mitochondria from *Hpdl*$^{-/-}$ pups and was improved by 4-HMA treatment (Fig. 3a). There was a non-statistically significant decrease in electron flow, rescued by 4-HMA, through complex IV (Fig. 3a). We observed similar decreases in electron flow through complexes I and II in mitochondria from the cortices of *Hpdl*$^{-/-}$ pups (Extended Data Fig. 6b). Mitochondria isolated from the cortices and cerebella of P90 *Hpdl*$^{-/-}$ mice treated with 4-HMA from P3 to P30 had electron flow through complexes I, II and IV comparable to that of P90 *Hpdl*$^{+/+}$ and *Hpdl*$^{+/-}$ mice (Extended Data Fig. 6c). 4-HMA treatment did not increase electron flow through complexes I, II or IV in mitochondria isolated from the cerebella of P12 *Hpdl*$^{+/+}$ pups (Extended Data Fig. 6d). These data demonstrate that loss of *Hpdl* attenuates electron flow through isolated cortex and cerebellar mitochondria in *Hpdl*$^{-/-}$ pups, presumably because of decreased CoQ levels. 4-HMA treatment

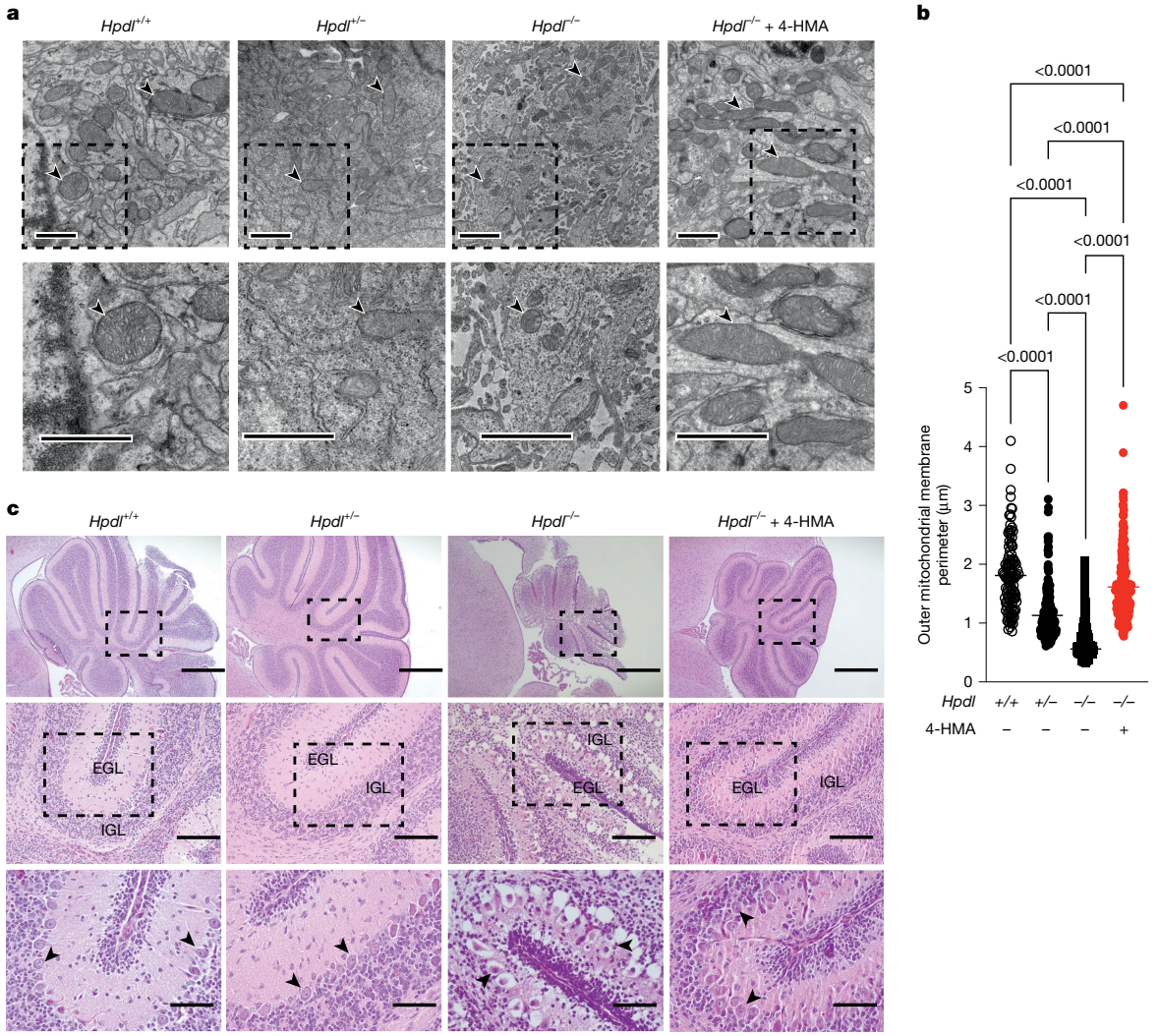


Fig. 2 | 4-HMA supplementation improves cerebellar histology in *Hpdl*$^{-/-}$ mice. a, Representative electron micrographs of the cerebella of P11 *Hpdl*$^{+/+}$, *Hpdl*$^{+/-}$ and *Hpdl*$^{-/-}$ mouse pups reveal significant changes in cerebellar mitochondrial morphology. The mitochondria (marked by arrowheads) in *Hpdl*$^{+/+}$ and *Hpdl*$^{+/-}$ mouse pups are intact, whereas those in the cerebella of *Hpdl*$^{-/-}$ mouse pups are fragmented. Supplementing *Hpdl*$^{-/-}$ mice with 10 mg kg^{-1} 4-HMA starting on P2–3 (*Hpdl*$^{-/-}$ + 4-HMA) restores cerebellar mitochondrial ultrastructure. Scale bars, 1 µm. **b**, Quantification of mitochondrial perimeter in electron micrographs of the cerebella of P11 *Hpdl*$^{+/+}$, *Hpdl*$^{+/-}$ and *Hpdl*$^{-/-}$ mouse pups as well as P11 *Hpdl*$^{-/-}$ mouse pups treated with 4-HMA. Mitochondria in the *Hpdl*$^{-/-}$ mouse pups are smaller than those of the *Hpdl*$^{+/+}$ and *Hpdl*$^{+/-}$ pups. 4-HMA treatment increases the size of the mitochondria in the *Hpdl*$^{-/-}$ pups, although not to the same size of mitochondria in *Hpdl*$^{+/+}$ pups. n = 117 (*Hpdl*$^{+/+}$), 227 (*Hpdl*$^{+/-}$), 677 (*Hpdl*$^{-/-}$) and 258 (*Hpdl*$^{-/-}$ + 4-HMA). **c**, P11 *Hpdl*$^{-/-}$ pups have marked cerebellar atrophy with PCs (arrowheads) showing vacuolization and intracellular oedema, thinning of the inner granular layer (IGL) and molecular layer and compaction of the external granular layer (EGL). These abnormalities are improved to near-wild-type morphology by supplementation with 4-HMA starting on P2–3 (*Hpdl*$^{-/-}$ + 4-HMA). Scale bars, 500 µm (top row); 125 µm (middle row); 62.5 µm (bottom row). Raw data and means are shown. *P* values are indicated on each plot. *P* values > 0.05 are not shown. For **b**, significance was tested by two-way ANOVA followed by Tukey's post hoc test.

from P3 to P30 restores electron flow through complexes I and II to near-wild-type levels even on P90. These data indicate that there is a CoQ threshold above which there is a durable rescue of mitochondrial electron flow, and that HPDL maintains CoQ pools above that threshold during development.

PCs are the sole output of the cerebellar cortex and depend on high metabolic activity to sustain rapid, chronic firing. To determine whether *Hpdl* loss affected the function of PCs, we manually patch-clamped PCs in brain slices from *Hpdl*$^{+/+}$ and *Hpdl*$^{+/-}$ mice, as well as untreated and 4-HMA-treated *Hpdl*$^{-/-}$ mice, in three age brackets: P8–10 pups (during cerebellar development), P17–19 pups (after cerebellar maturation was mostly completed)[31] and P56–57 pups (the age at which we did our behavioural studies). The P17–19 and P56–57 groups did not have untreated *Hpdl*$^{-/-}$ pups as these animals die by P15. In the P8–10 group, PCs from *Hpdl*$^{-/-}$ mice had increased input resistance (R_i) compared with PCs from *Hpdl*$^{+/+}$ and *Hpdl*$^{+/-}$ mice (Fig. 3b and Table 1), indicative of fewer membrane ion channels. There was a significant reduction in membrane capacitance (C_m) in *Hpdl*$^{-/-}$ PCs relative to *Hpdl*$^{+/-}$ PCs[32,33], indicative of smaller or less developed cells (Fig. 3b). These electrophysiological deficits were partially restored by 4-HMA treatment such that R_i was comparable to that of PCs of *Hpdl*$^{+/-}$ mice and lower than the R_i of PCs from *Hpdl*$^{+/+}$ mice (Fig. 3b). Moreover, the C_m of PCs from 4-HMA-treated *Hpdl*$^{-/-}$ mice significantly increased relative to that of PCs from *Hpdl*$^{-/-}$ mice and was higher than that of PCs from *Hpdl*$^{+/+}$ and *Hpdl*$^{+/-}$ mice (Fig. 3b). By P17–19 or P56–57, no differences were observed in the R_i and C_m of PCs from *Hpdl*$^{+/+}$, *Hpdl*$^{+/-}$ and *Hpdl*$^{-/-}$ pups treated with 4-HMA (Fig. 3c, Table 1 and Extended Data Fig. 7h). These data are consistent with 4-HMA treatment correcting the aberrant passive electrophysiological characteristics of cerebellar PCs from *Hpdl*$^{-/-}$ pups.

We next tested whether *Hpdl* loss affected the current–voltage (I–V) curves of PCs in mouse pups. Cerebellar PCs from P8–10 *Hpdl*$^{-/-}$ pups had a tighter grouping of currents at hyperpolarized membrane

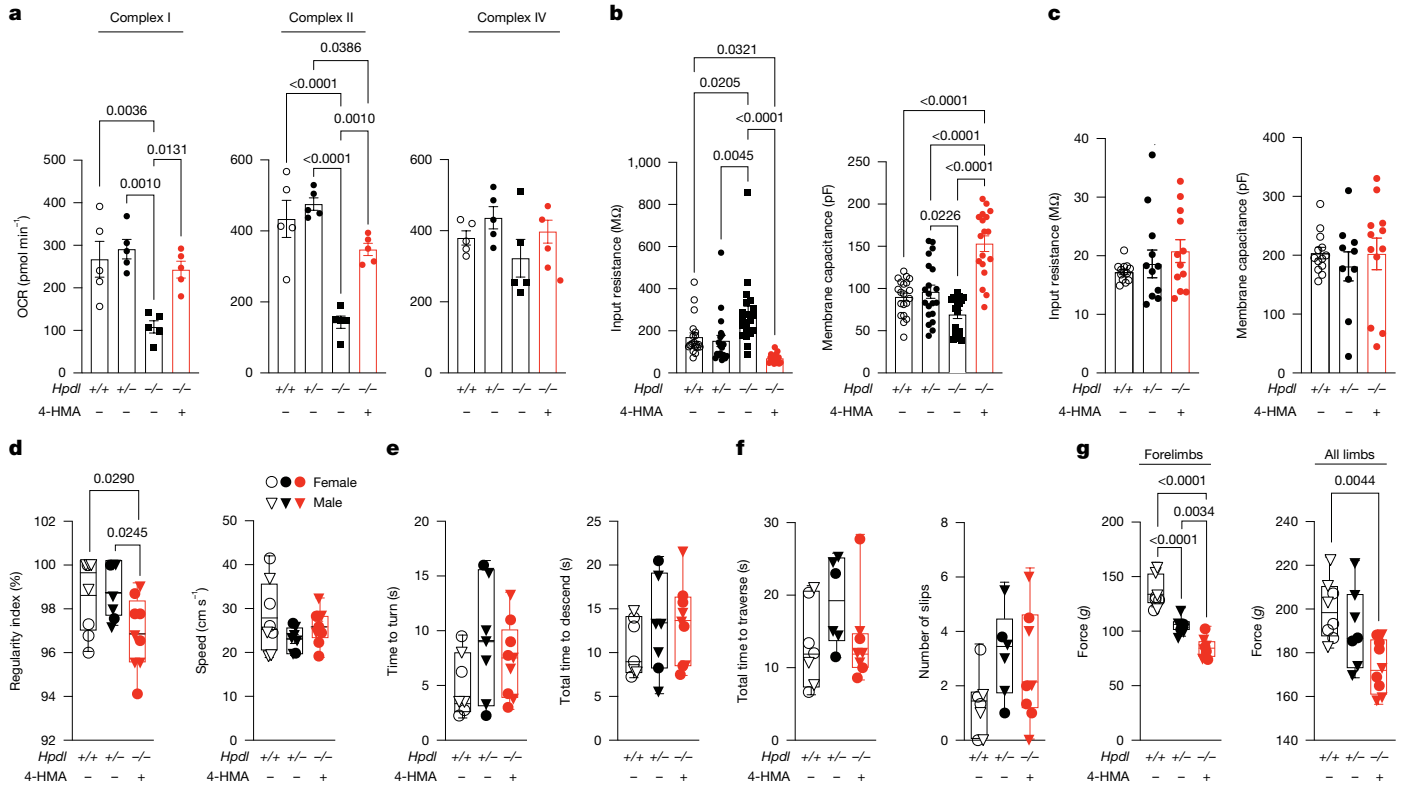


Fig. 3 | 4-HMA improves PC function and behavioural phenotypes of *Hpdl*$^{-/-}$ mice. a, Electron flow in cerebellar mitochondria from P9 *Hpdl*$^{+/+}$, *Hpdl*$^{+/-}$ and *Hpdl*$^{-/-}$ pups as well as P9 4-HMA-treated *Hpdl*$^{-/-}$ pups. Electron flow through complexes I and II is impaired in *Hpdl*$^{-/-}$ mice and is restored by 4-HMA treatment. There was a non-statistically significant decrease in electron flow, rescued by 4-HMA, through complex IV. $n = 5$ animals for all groups. **b**, Patch-clamping of PCs in brain slices from P8–10 pups increases input resistance and decreases membrane capacitance in PCs from *Hpdl*$^{-/-}$ pups relative to PCs from *Hpdl*$^{+/+}$ and *Hpdl*$^{+/-}$ pups. (*Hpdl*$^{+/+}$, $n = 20$; *Hpdl*$^{+/-}$, $n = 20$; *Hpdl*$^{-/-}$, $n = 20$; 4-HMA-treated *Hpdl*$^{-/-}$, $n = 18$). **c**, 4-HMA supplementation restores input resistance and membrane capacitance of PCs from *Hpdl*$^{-/-}$ pups to levels comparable to those in *Hpdl*$^{+/+}$ and *Hpdl*$^{+/-}$ pups on P17–19. (*Hpdl*$^{+/+}$, $n = 13$; *Hpdl*$^{+/-}$, $n = 10$; 4-HMA-treated *Hpdl*$^{-/-}$, $n = 12$). **d**, 4-HMA-treated 8–10-week-old *Hpdl*$^{-/-}$ mice have reduced gait regularity relative to *Hpdl*$^{+/+}$ and *Hpdl*$^{+/-}$ mice. There were no differences in gait speed between the groups. **e**,**f**, 4-HMA-treated 8–10-week-old *Hpdl*$^{-/-}$ mice have similar performance to *Hpdl*$^{+/+}$ and *Hpdl*$^{+/-}$ mice in the pole test (**e**) and the transverse beam test (**f**). **g**, Forelimb grip strength (left) is decreased in 8–10-week-old *Hpdl*$^{+/-}$ and 4-HMA-treated *Hpdl*$^{-/-}$ mice relative to *Hpdl*$^{+/+}$ mice. All-limb grip strength (right) is similar in all groups. For behavioural tests, data from male mice (n: *Hpdl*$^{+/+}$ = 4, *Hpdl*$^{+/-}$ = 5, 4-HMA-treated *Hpdl*$^{-/-}$ = 4) are plotted as triangles. Data from female mice (n: *Hpdl*$^{+/+}$ = 4, *Hpdl*$^{+/-}$ = 2, 4-HMA-treated *Hpdl*$^{-/-}$ = 5) are plotted as circles. Behavioural data do not include untreated *Hpdl*$^{-/-}$ mice. Data are mean ± s.e.m. as well as raw data. For box-and-whisker plots, the centre is the median, the box bounds are the 25th to 75th percentiles and whiskers indicate minimum to maximum. Significance was tested by two-way ANOVA with Tukey's post hoc test.

potentials (−100 to −60 mV) relative to that of *Hpdl*$^{+/+}$ PCs (Extended Data Fig. 7a, insets), resulting in a flatter *I*–*V* curve for *Hpdl*$^{-/-}$ PCs at hyperpolarized membrane potentials (Extended Data Fig. 7a). Interestingly, 4-HMA treatment seemed to overcompensate for this, resulting in a steeper *I*–*V* curve of PCs in *Hpdl*$^{-/-}$ pups relative to those of the other groups (Extended Data Fig. 7a), closer in slope and magnitude to the *I*–*V* curves of P17–19 PCs (Extended Data Fig. 7b). The *I*–*V* curves of PCs from P17–19 and P56–57 *Hpdl*$^{+/+}$, *Hpdl*$^{+/-}$ and 4-HMA-treated *Hpdl*$^{-/-}$ pups were comparable (Extended Data Fig. 7b,c). These data are consistent with PCs from *Hpdl*$^{-/-}$ pups having differential sensitivity to inputs at hyperpolarized membrane potentials than do *Hpdl*$^{+/+}$ and *Hpdl*$^{+/-}$ PCs and partial reversion of these electrophysiological properties by 4-HMA.

The peak frequency of PCs from P8–10 *Hpdl*$^{-/-}$ pups was significantly lower than those of *Hpdl*$^{+/+}$ and *Hpdl*$^{+/-}$ PCs but was increased by 4-HMA treatment to a level higher than that of *Hpdl*$^{+/+}$ pups (Extended Data Fig. 7d). These differences resolved by P17–19 (Extended Data Fig. 7e). These findings are consistent with *Hpdl*$^{-/-}$ PCs being immature relative to PCs of *Hpdl*$^{+/+}$ and *Hpdl*$^{+/-}$ pups and the maturation of 4-HMA-treated *Hpdl*$^{-/-}$ PCs being accelerated. *Hpdl* loss and 4-HMA rescue did not affect the firing rate–current curves of PCs from P7–10 or 17–19 pups (Extended Data Fig. 7f,g). However, PCs from P56–57 *Hpdl*$^{+/+}$ mice had a higher firing rate at higher input currents than PCs from *Hpdl*$^{+/-}$ and 4-HMA-treated *Hpdl*$^{-/-}$ mice (Extended Data Fig. 7i). Likewise, action-potential parameters of PCs from *Hpdl*$^{+/+}$, *Hpdl*$^{+/-}$ and *Hpdl*$^{-/-}$ pups were mostly similar (Extended Data Fig. 8a). However, spike thresholds of PCs from *Hpdl*$^{-/-}$ pups treated with 4-HMA were more hyperpolarized than those of PCs from *Hpdl*$^{+/+}$, *Hpdl*$^{+/-}$ and untreated *Hpdl*$^{-/-}$ pups on P8–10 (Extended Data Fig. 8a). The action half potential and spike half-width of PCs from *Hpdl*$^{-/-}$ pups treated with 4-HMA were slightly less than those of PCs from *Hpdl*$^{+/+}$ pups (Extended Data Fig. 8a). The differences in action half potential between PCs from *Hpdl*$^{+/+}$ or untreated *Hpdl*$^{-/-}$ pups and those from *Hpdl*$^{-/-}$ pups treated with 4-HMA persisted on P17–19 (Extended Data Fig. 8b). No significant differences in peak frequency or action-potential characteristics in PCs from P56–57 (8-week-old) *Hpdl*$^{+/+}$, *Hpdl*$^{+/-}$ and 4-HMA-treated *Hpdl*$^{-/-}$ mice were observed (Extended Data Fig. 8c).

These results demonstrate that homozygous *Hpdl* loss delays the functional maturation of cerebellar PCs. 4-HMA treatment accelerates and ultimately restores the functional maturity of cerebellar PCs as measured by electrophysiological parameters.

4-HMA treats *Hpdl*$^{-/-}$ motor symptoms in pups

Patients with *HPDL* variants typically present with ataxia, spastic tetraplegia and other deficits in motor function. To test whether 4-HMA

Table 1 | Passive electrophysiological characteristics of cerebellar PCs

	Hpdl$^{+/+}$	*Hpdl*$^{+/-}$	*Hpdl*$^{-/-}$	*Hpdl*$^{-/-}$+4-HMA
R_i (MΩ)				
P8–9	170.5±20.14	152.6±26.22	274.4±35.61	69.8±5.16
P17–19	17.2±0.43	18.6±2.37	–	20.8±1.96
P56–57	16.11±1.22	12.24±1.87	–	16.78±1.29
C_m (pF)				
P8–9	90.0±4.74	96.2±7.85	68.3±4.82	153.1±9.24
P17–19	203.6±9.77	181.2±24.8	–	202.5±26.83
P56–57	189.8±14.52	244.23±26.04	–	180.96±19.69

No data are available for the groups indicated by –, because the mice die by P15.

improved the metabolic physiology and neurological symptoms associated with *Hpdl* variants, we carried out metabolic home-cage measurements and tests of motor function on P58 (approximately 8-week-old) *Hpdl*$^{-/-}$ mice treated with 4-HMA and compared them with *Hpdl*$^{+/+}$ and *Hpdl*$^{+/-}$ mice. 4-HMA reduced seizures in *Hpdl*$^{-/-}$ mice (Extended Data Fig. 1b). At the start of testing, male, but not female, *Hpdl*$^{-/-}$ mice weighed less than their *Hpdl*$^{+/+}$ and *Hpdl*$^{+/-}$ counterparts (Extended Data Fig. 9c) but had no significant differences in food or water consumption, activity, maximal oxygen consumption, carbon dioxide production or energy expenditure (Extended Data Fig. 9a). *Hpdl*$^{-/-}$ male, but not female, mice treated with 4-HMA had a significantly elevated respiratory exchange ratio (RER) compared with *Hpdl*$^{+/-}$ and *Hpdl*$^{+/+}$ mice (sex × genotype interaction: $F_{2,17} = 9.913$, $P < 0.01$), suggestive of altered energy substrate use (Extended Data Fig. 9b,d). This effect seemed to be gene-dosage dependent, as *Hpdl*$^{+/-}$ male mice had statistically intermediate RER values (male *Hpdl*$^{+/-}$ versus *Hpdl*$^{+/+}$, $P < 0.05$; male *Hpdl*$^{+/-}$ versus *Hpdl*$^{-/-}$, $P < 0.05$; Extended Data Fig. 9b,d). *Hpdl*$^{-/-}$ mice treated with 4-HMA had a mild, significant reduction in the regularity of their step sequence ($F_{2,17} = 3.826$, $P < 0.05$; Fig. 3d). The first-order effect of the gait analysis was mouse survival that enabled ambulation. However, 4-HMA-treated *Hpdl*$^{-/-}$ mice showed no significant impairments in any other gait parameter or in the open-field, rotarod, pole and transverse-beam tests, which assess motor learning, coordination and balance (Fig. 3e,f, Extended Data Figs. 9e,f and 10a and Supplementary Videos 3–5). A gene-dosage effect was observed in forelimb grip strength, with significant reductions found in 4-HMA-treated *Hpdl*$^{-/-}$ mice relative to *Hpdl*$^{+/-}$ and *Hpdl*$^{+/+}$ mice ($F_{2,17} = 38.908$, $P < 0.001$), and with *Hpdl*$^{+/-}$ mice having significantly lower forelimb grip strength than *Hpdl*$^{+/+}$ mice (Fig. 3g). This pattern was similar but less pronounced in measures averaging grip strength for all four limbs. Only *Hpdl*$^{-/-}$ mice treated with 4-HMA had significant reductions in grip strength relative to *Hpdl*$^{+/+}$ mice ($F_{2,17} = 4.358$, $P < 0.05$; Fig 3g). These results are potentially consistent with the firing rate–current curves of PCs from P56–57 *Hpdl*$^{+/-}$ mice and 4-HMA-treated *Hpdl*$^{-/-}$ mice, which have lower firing rates at higher input currents than do PCs from P56–57 *Hpdl*$^{+/+}$ mice (Extended Data Fig. 7i).

The gene-dosage effects on RER in male mice and on mouse grip strength suggest that there are neurological and metabolic features affected by *Hpdl* loss that are partially restored by our current 4-HMA treatment regimen, indicating that treatment may need optimization or that some neurological features are refractory to 4-HMA treatment. However, the improvement of motor phenotypes in 4-HMA-treated *Hpdl*$^{-/-}$ mice suggests that 4-HMA could improve the outcomes of humans with neurological symptoms due to *HPDL* variants.

4-HB can treat a patient with *HPDL* encephalopathy

An eight-year-old child with biallelic *HPDL* variants (c.3G>C (p.Met1Ile), c.789delG (p.P264Lfs*51)) had a healthy birth and healthy development until eight years of age, when he presented with rapidly progressing spasticity over 2–3 months, although he probably had subtle symptoms before then. The child was able to run and participate in typical sports in August 2023, developed bilateral ankle clonus in September 2023 and could no longer run or participate in typical sports in October 2023. He was started on systemic CoQ_{10} supplementation in mid-October 2023. In early November 2023, medical records note that he could stand without support but had difficulty maintaining an upright posture with feet together. By late November 2023, he fell frequently and his ambulation was impaired to the degree that physical therapists advised the family to obtain a wheelchair. The patient's family history included two younger siblings who had died in infancy (Fig. 4a), and who both developed rapidly progressing and catastrophic encephalopathy and seizures. The second sibling received genetic testing, revealing biallelic *HPDL* variants (c.3G>C (p.Met1Ile), c.789delG (p.P264Lfs*51)). After the onset of symptoms in the eight-year-old child, genetic testing confirmed the same biallelic variants. Both variants are reported in ClinVar[34] as pathogenic (VCV001344855.5 and VCV002221909.2) and the association of the c.3G>C (p.Met1Ile) variant with NEDSWMA has previously been reported[19]. *HPDL* variants are ultra-rare based on calculated allele frequencies (Table 2).

Given the rapid and apparently unrelenting progression of the patient's symptoms (including 1.5 months while the patient was taking CoQ_{10}), the history of a sibling with NEDSWMA and the availability of 4-HB in highly pure form, we proposed treatment with 4-HB. The administration of 4-HB was approved by the US Food and Drug Administration (single patient investigational new drug (IND) 170119) and the treatment protocol was approved by the NYU institutional review board (IRB; protocol 23-01512). The parents provided informed consent and the

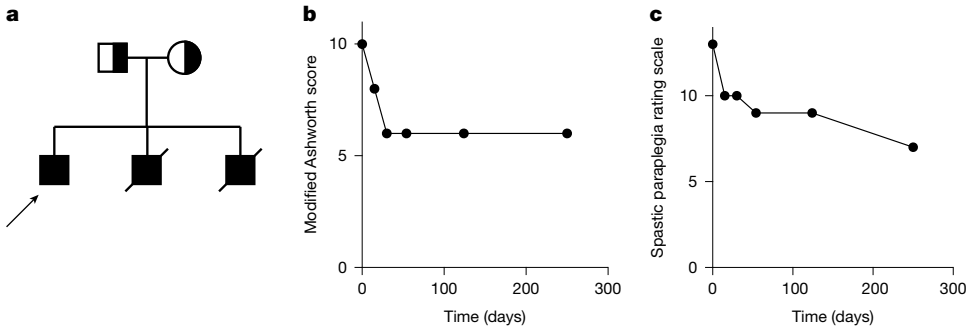


Fig. 4 | Treatment of a single patient with *HPDL* encephalopathy with the CoQ_{10} headgroup intermediate 4-HB. a, Pedigree of a patient with biallelic *HPDL* variants treated with 4-HB. The patient had two older siblings who died in infancy, the second child shared the same genotype. **b**, Decrease in the modified Ashworth score, a validated measure of spasticity, over the initial treatment course. Lack of spasticity = 0. Mitochondrial diseases generally have stable or increased Modified Ashworth scores over time. **c**, Decrease in the SPRS, a measure of spasticity and its effects on quality of life, over the treatment course to date. Mitochondrial diseases generally have stable or increased SPRS scores over time.

Table 2 | Allele frequency data for *HPDL* variants

	Allele frequency	Chance of homozygous variant	Incidence (1 per *n*)	Number in the USA	Number worldwide
Benign	2.0×10^{-3}	–	–	–	–
Likely benign	8.6×10^{-4}	–	–	–	–
Likely pathogenic	2.3×10^{-4}	5.2×10^{-8}	19,308,211	17	409
Pathogenic	8.0×10^{-5}	6.4×10^{-9}	155,183,640	2	51
Likely pathogenic (upper bound)	3.4×10^{-3}	1.2×10^{-5}	86,319	3,835	91,382
Likely pathogenic (lower bound)	5.3×10^{-4}	2.8×10^{-7}	3,581,219	92	2,203
Uncertain significance	8.5×10^{-5}	7.2×10^{-9}	138,283,577	2	57

Data are from GnomAD[43].

child agreed to treatment with 4-HB; data are shared with permission. Initial assessments included a brain MRI, with scans showing patchy T2 hyperintensity of the corticospinal tract of unclear relevance and no major cerebellar abnormalities (Extended Data Fig. 10b).

The patient started treatment with 30 mg of 4-HB in a 5 mg ml^{-1} solution (6 ml) in water on day 1. On the basis of preclinical data, the dose was rapidly increased over the first 4 days to 100 mg kg^{-1} (600 ml of solution); that dose was maintained until day 30 of treatment. The dose was then decreased to 50 mg kg^{-1} (300 ml of solution) for an additional 95 days and then decreased to the current dose of 25 mg kg^{-1}. The child generally tolerated the treatment well; the solution was palatable and was reported to have a sour taste. During the first 30 days of the study, on several occasions, the child had emesis shortly after drinking the 600 ml solution, attributed to the large volume of solution ingested over a short period of time (15–20 min). No further emesis occurred during the 30 days with the lower dose volume of 300 ml. Safety monitoring, including electrocardiograms and bloodwork, was reassuring; there was no substantial change in these values for the duration of treatment. The data presented include 250 days of treatment. CoQ_{10} was discontinued after several months of treatment with 4-HB.

Outcome measures (Table 3) demonstrate improvement of spasticity according to the modified Ashworth score[35] with the sum total of scores decreasing from 10 to 6 (Fig. 4b). The spastic paraplegia rating scale (SPRS)[36] score, a measure of spasticity and its effects on quality of life, improved from 13 to 7 (Fig. 4c). Scores for the nine-hole peg test[37], a measure of hand–finger dexterity, are consistent with stabilization or subtle improvement of the child's hand movement to times typical for children his age (Table 3). The 10-m walk test[38] results are varied, in part because the child compensated for profound imbalance with increased walking speed at the beginning of the study. The patient's brain MRI did not change after 30 days of treatment (Extended Data Fig. 10b). Subjective reports, some of which are components of the SPRS, include improvement in endurance (the patient initially struggled to walk across a hospital lobby and by 30 days walked for 20 min), improvement in balance (the patient initially was unable to stand in tandem and was able to do so about 2 weeks

Table 3 | Clinical outcomes for a patient with *HPDL* encephalopathy treated with 4-HB

Clinical outcome	Day 0	Day 15	Day 30	Day 54	Day 124	Day 250
Modified Ashworth score total	10	8	6	6	6	6
Arm extension, right	0	0	0	0	0	0
Arm extension, left	0	0	0	0	0	0
Hip adduction, right	1	1	1	1	1	1
Hip adduction, left	1	1	1	1	1	1
Hip flexion, right	1	1	0	0	0	0
Hip flexion, left	1	1	0	0	0	0
Knee extension, right	2	1	1	1	1	1
Knee extension, left	2	1	1	1	1	1
Ankle, right	1 (clonus)	1 (clonus)	1 (clonus)	1 (clonus)	1 (clonus)	1 (clonus)
Ankle, left	1 (clonus)	1 (clonus)	1 (clonus)	1 (clonus)	1 (clonus)	1 (clonus)
SPRS	13	10	10	9	9	7
Nine-hole peg test, right (dominant) hand, trial 1	29.6	23.5	19.8	20.9	19.2	19.7
Nine-hole peg test, right (dominant) hand, trial 2	22.6	20.6	24.4	21.9	21.1	17.3
Nine-hole peg test, left (non-dominant) hand, trial 1	33.2	31.2	23.5	24.2	21.8	20.1
Nine-hole peg test, left (non-dominant) hand, trial 2	29.2	23.5	28.0	21.6	24.2	22.2
10-m walk, first attempt (s)	6.3	7.2	6.1	8.3	7.8	9.6
10-m walk, second attempt (s)	6.2	7.2	5.8	8.0	7.4	10.2
10-m walk with turn, walk back (s)	14.9	14.7	12.2	15.5	14.3	19.4

NA,

Table 4 | Patient-reported outcomes for a patient with *HPDL* encephalopathy treated with 4-HB

Patient-reported outcomes	Day 2	Day 12	Day 30	Day 54	Day 124	Day 250
Stance with one foot forward (time (s) for right, left)	57, 60	190, 190	*	*	NA	NA
Tandem stance (time (s) for right, left)	Unable	21, 30	*	*	NA	NA
Falls	Daily	Daily	Weekly	Weekly	Rare	Rare
Able to run	No	No	No	Yes	Yes	Yes
Able to ride a bicycle	No	No	No	No	Yes	Yes
Able to step laterally to catch a ball	No	No	No	No	No	Yes

*Not quantified as the patient became bored and started walking after standing for 3 min (one foot forward) or 30 s (tandem stance).

after treatment initiation; after 8 months of treatment he was able to step laterally to catch a ball), decreased fall frequency from multiple times daily to rarely and restoration of running by approximately 1.5 months of treatment (Table 4).

These data and observations demonstrate the safety and tolerance of 4-HB treatment in a child at a dose of 100 mg kg^{-1} for 27 treatments, followed by 50 mg kg^{-1} for 95 treatments and subsequent treatment with a maintenance dose of 25 mg kg^{-1}. We show stabilization over the course of a rapidly progressing spasticity, followed by objective and subjective improvement in the child's motor function, providing evidence of improvement in neurological symptoms in a patient with *HPDL* encephalopathy[17–23,39,40].

Discussion

The central role of CoQ_{10} in mitochondrial health has long been understood. Attempts to improve CoQ_{10} synthesis have been difficult in the periphery[41] and impossible in the central nervous system. Here we demonstrate that the CoQ_{10} headgroup intermediates 4-HMA and 4-HB efficiently rescue the neurological phenotypes of *Hpdl*$^{-/-}$ mice, which model an ultra-rare primary CoQ_{10} deficiency. 4-HB modified the course of an *HPDL*-variant mitochondrial disease in a patient with no toxicity during eight months of treatment. Our results demonstrate that the mammalian CoQ_{10} synthesis pathway is amenable to pharmacological repletion with CoQ_{10} headgroup intermediates. We demonstrate that metabolite-replacement therapy improves the neurological symptoms of a primary CoQ_{10} deficiency in a patient.

Although 4-HMA treatment improves most neurological deficits and improves the survival of *Hpdl*$^{-/-}$ mice when administered by day 6 or 7 postnatally, initiation of treatment after P10 did not improve *Hpdl*$^{-/-}$ pup survival. These data indicate that there is a critical window in neural development during which the effects of *HPDL* encephalopathy will be partially reversible in patients. Treatment with CoQ_{10} headgroup intermediates during the critical window restores cellular function and development and improves neurological symptoms, even though our current 4-HMA and 4-HB treatment regimen only partially restores CoQ pools in the brains of *Hpdl*$^{-/-}$ mice. Patients, such as the person we treated, may have a longer critical window if they retain any residual HPDL activity. Once brain development is complete[42], CoQ_{10} headgroup synthesis might be dispensable. In support of this hypothesis, 4-HMA-treated *Hpdl*$^{-/-}$ mice survive without supplementation of CoQ_{10} headgroup intermediates after P30.

The durable rescue of mitochondrial function in *Hpdl*$^{-/-}$ mice suggests a CoQ threshold effect as well as differential requirements for CoQ synthesis during development and in adulthood. CoQ headgroup synthesis may not be required for the survival of adult mice living under controlled conditions, particularly if there are alternative sources of CoQ or CoQ headgroups. Conditional deletion of *Hpdl* will enable us to address the tissue-specific and temporal requirements of HPDL activity.

Loss of CoQ headgroup synthesis is associated with increased TUNEL staining, consistent with apoptosis, in the developing cerebellum and in the cortex, striatum and thalamus (Extended Data Figs. 3b,d and 5a). This may be caused by loss of mitochondrial function or increased mitochondrial or cellular reactive oxygen species due to decreased CoQ. Increased apoptosis in these brain regions may contribute to the clinical symptoms of patients with *HPDL* variants. Determining the mechanisms underlying increased sensitivity of specific brain regions to loss of HPDL and CoQ headgroup synthesis will require further research.

Treatment with $^{13}C_6$-4-HMA or 4-HB restores CoQ_9 and CoQ_{10} pools in *Hpdl*$^{-/-}$ mice to about half that of wild-type mice and a significant fraction of CoQ_9 and CoQ_{10} remains unlabelled. These results are consistent with a parallel CoQ headgroup synthesis pathway or the uptake of CoQ headgroup from maternal milk, diet or another source. This alternative pathway is not sufficient for development but enables the survival of mice once development is complete. An alternative source of CoQ_{10} headgroup intermediates (or CoQ_{10} itself) may account for some of the variability in the presentation of HPDL encephalopathy and other primary CoQ_{10} deficiencies. Surprisingly, lower CoQ_9 and CoQ_{10} levels restore mitochondrial electron flow and improve the survival of *Hpdl*$^{-/-}$ mice, although lower CoQ levels may be responsible for the reduced grip strength of 4-HMA-treated *Hpdl*$^{-/-}$ mice. Additional studies will be needed to test whether prenatal treatment, higher doses and improved formulations of 4-HMA and 4-HB increase brain CoQ_9 and CoQ_{10} pools to wild-type levels. Our data are consistent with a role of HPDL in controlling the amount of CoQ_9 and CoQ_{10} in the brain.

Oral administration of 4-HB at high doses rescues perinatal lethality in mice with hypomorphic *Coq2*, which conjugates 4-HB to its isoprenoid tail during CoQ_{10} synthesis[16]. This previous work indicates that CoQ_{10} headgroup intermediates could treat other primary CoQ_{10} deficiencies. The authors of this previous work suggested that the treatment of *HPDL* pathogenic variants with 4-HB would require further investigation. Here we demonstrate that both 4-HMA and 4-HB restore the growth of mice lacking *Hpdl* and that 4-HB can improve the clinical outcomes of a child with a neurodevelopmental disorder driven by *HPDL* variants. We anticipate that early treatment with 4-HMA or 4-HB, enabled by newborn screening tests to detect inborn errors in CoQ_{10} headgroup synthesis or conjugation, will maximize the therapeutic benefits of treatment with CoQ_{10} headgroup intermediates. Larger trials of CoQ_{10} headgroup replacement therapy in patients with *HPDL* variants will be required to determine the outcomes of treatment with CoQ_{10} headgroup intermediates.

Online content

Any methods, additional references, Nature Portfolio reporting summaries, source data, extended data, supplementary information, acknowledgements, peer review information; details of author contributions and competing interests; and statements of data and code availability are available at https://doi.org/10.1038/s41586-025-09246-x.

1. Emmanuele, V. et al. Heterogeneity of coenzyme Q10 deficiency: patient study and literature review. *Arch. Neurol.* **69**, 978–983 (2012).
2. Bersuker, K. et al. The CoQ oxidoreductase FSP1 acts parallel to GPX4 to inhibit ferroptosis. *Nature* **575**, 688–692 (2019).
3. Awad, A. M. et al. Coenzyme Q_{10} deficiencies: pathways in yeast and humans. *Essays Biochem.* **62**, 361–376 (2018).
4. Mantle, D., Millichap, L., Castro-Marrero, J. & Hargreaves, I. P. Primary coenzyme Q10 deficiency: an update. *Antioxidants* **12**, 1652 (2023).
5. Stefely, J. A. & Pagliarini, D. J. Biochemistry of mitochondrial coenzyme Q biosynthesis. *Trends Biochem. Sci.* **42**, 824–843 (2017).
6. Guerra, R. M. & Pagliarini, D. J. Coenzyme Q biochemistry and biosynthesis. *Trends Biochem. Sci.* **48**, 463–476 (2023).
7. Banh, R. S. et al. The polar oxy-metabolome reveals the 4-hydroxymandelate CoQ10 synthesis pathway. *Nature* **597**, 420–425 (2021).

8. Quinzii, C. M. & Hirano, M. Primary and secondary CoQ_{10} deficiencies in humans. *Biofactors* **37**, 361–365 (2011).
9. Mas, E. & Mori, T. A. Coenzyme Q_{10} and statin myalgia: what is the evidence? *Curr. Atheroscler. Rep.* **12**, 407–413 (2010).
10. Bentinger, M. et al. Stimulation of coenzyme Q synthesis. *Biofactors* **32**, 99–111 (2008).
11. Wang, Y., Oxer, D. & Hekimi, S. Mitochondrial function and lifespan of mice with controlled ubiquinone biosynthesis. *Nat. Commun.* **6**, 6393 (2015).
12. Freyer, C. et al. Rescue of primary ubiquinone deficiency due to a novel *COQ7* defect using 2,4-dihydroxybensoic acid. *J. Med. Genet.* **52**, 779–873 (2015).
13. Wang, Y. et al. Pathogenicity of two *COQ7* mutations and responses to 2,4-dihydroxybenzoate bypass treatment. *J. Cell. Mol. Med.* **21**, 2329–2343 (2017).
14. Wang, Y. & Hekimi, S. The efficacy of coenzyme Q_{10} treatment in alleviating the symptoms of primary coenzyme Q_{10} deficiency: a systematic review. *J. Cell. Mol. Med.* **26**, 4635–4644 (2022).
15. Fernández-del-Río, L. & Clarke, C. F. Coenzyme Q biosynthesis: an update on the origins of the benzenoid ring and discovery of new ring precursors. *Metabolites* **11**, 385 (2021).
16. Corral-Sarasa, J. et al. 4-Hydroxybenzoic acid rescues multisystemic disease and perinatal lethality in a mouse model of mitochondrial disease. *Cell Rep.* **43**, 114148 (2024).
17. Husain, R. A. et al. Bi-allelic HPDL variants cause a neurodegenerative disease ranging from neonatal encephalopathy to adolescent-onset spastic paraplegia. *Am. J. Hum. Genet.* **107**, 364–373 (2020).
18. Sun, Y. et al. HPDL deficiency causes a neuromuscular disease by impairing the mitochondrial respiration. *J. Genet. Genomics* **48**, 727–736 (2021).
19. Wiessner, M. et al. Biallelic variants in HPDL cause pure and complicated hereditary spastic paraplegia. *Brain* **144**, 1422–1434 (2021).
20. Morgan, N. V. et al. Evidence that autosomal recessive spastic cerebral palsy-1 (CPSQ1) is caused by a missense variant in *HPDL*. *Brain Commun.* **3**, fcab002 (2021).
21. Ghosh, S. G. et al. Biallelic variants in *HPDL*, encoding 4-hydroxyphenylpyruvate dioxygenase-like protein, lead to an infantile neurodegenerative condition. *Genet. Med.* **23**, 524–533 (2021).
22. Yu, H., Wei, Q., Luo, W.-J. & Wu, Z.-Y. Novel bi-allelic *HPDL* variants cause hereditary spastic paraplegia in a Chinese patient. *Clin. Genet.* **100**, 777–778 (2021).
23. Micule, I. et al. Case report: two families with *HPDL* related neurodegeneration. *Front. Genet.* **13**, 780764 (2022).
24. Mancuso, M., Orsucci, D., Volpi, L., Calsolaro, V. & Siciliano, G. Coenzyme Q10 in neuromuscular and neurodegenerative disorders. *Curr. Drug Targets* **11**, 111–121 (2010).
25. López, L. C. et al. Treatment of CoQ_{10} deficient fibroblasts with ubiquinone, CoQ analogs, and vitamin C: time- and compound-dependent effects. *PLoS ONE* **5**, e11897 (2010).
26. Dare, A. J. et al. Protection against renal ischemia–reperfusion injury in vivo by the mitochondria targeted antioxidant MitoQ. *Redox Biol.* **5**, 163–168 (2015).
27. Albano, C. B., Muralikrishnan, D. & Ebadi, M. Distribution of coenzyme Q homologues in brain. *Neurochem. Res.* **27**, 359–368 (2002).
28. Tran, U. C. & Clarke, C. F. Endogenous synthesis of coenzyme Q in eukaryotes. *Mitochondrion* **7**, S62–S71 (2007).
29. Stefely, J. A. et al. Cerebellar ataxia and coenzyme Q deficiency through loss of unorthodox kinase activity. *Mol. Cell* **63**, 608–620 (2016).
30. Naini, A., Lewis, V. J., Hirano, M. & Dimauro, S. Primary coenzyme Q10 deficiency and the brain. *Biofactors* **18**, 145–152 (2003).
31. Millen, K. J., Wurst, W., Herrup, K. & Joyner, A. L. Abnormal embryonic cerebellar development and patterning of postnatal foliation in two mouse Engrailed-2 mutants. *Development* **120**, 695–706 (1994).
32. Hockberger, P. E., Tseng, H. Y. & Connor, J. A. Development of rat cerebellar Purkinje cells: electrophysiological properties following acute isolation and in long-term culture. *J. Neurosci.* **9**, 2258–2271 (1989).
33. Arancillo, M., White, J. J., Lin, T., Stay, T. L. & Sillitoe, R. V. In vivo analysis of Purkinje cell firing properties during postnatal mouse development. *J. Neurophysiol.* **113**, 578–591 (2015).
34. Landrum, M. J. et al. ClinVar: public archive of interpretations of clinically relevant variants. *Nucleic Acids Res.* **44**, D862–D868 (2016).
35. Meseguer-Henarejos, A.-B., Sánchez-Meca, J., López-Pina, J.-A. & Carles-Hernández, R. Inter- and intra-rater reliability of the Modified Ashworth Scale: a systematic review and meta-analysis. *Eur. J. Phys. Rehabil. Med.* **54**, 576–590 (2018).
36. Schüle, R. et al. The Spastic Paraplegia Rating Scale (SPRS): a reliable and valid measure of disease severity. *Neurology* **67**, 430–434 (2006).
37. Wang, Y.-C., Bohannon, R. W., Kapellusch, J., Garg, A. & Gershon, R. C. Dexterity as measured with the 9-Hole Peg Test (9-HPT) across the age span. *J. Hand Ther.* **28**, 53–60 (2015).
38. de Baptista, C. R. J. A. et al. Methods of 10-meter walk test and repercussions for reliability obtained in typically developing children. *Rehabil. Res. Pract.* **2020**, 4209812 (2020).
39. Kojima, F. et al. A novel homozygous *HPDL* variant in Japanese siblings with autosomal recessive hereditary spastic paraplegia: case report and literature review. *Neurogenetics* **25**, 149–156 (2024).
40. Ma, Y. et al. Two novel heterozygous *HPDL* variants in a Chinese family with a neurodevelopmental disorder with progressive spasticity and brain white matter abnormalities. *Gene* **934**, 149018 (2025).
41. Yogev, Y. et al. Limb girdle muscular disease caused by *HMGCR* mutation and statin myopathy treatable with mevalonolactone. *Proc. Natl Acad. Sci.* **120**, e2217831120 (2023).
42. Pujol, J., Vendrell, P., Junqué, C., Martí-Vilalta, J. L. & Capdevila, A. When does human brain development end? Evidence of corpus callosum growth up to adulthood. *Ann. Neurol.* **34**, 71–75 (1993).
43. Karczewski, K. J. et al. The mutational constraint spectrum quantified from variation in 141,456 humans. *Nature* **581**, 434–443 (2020).

Publisher's note Springer Nature remains neutral with regard to jurisdictional claims in published maps and institutional affiliations.

Springer Nature or its licensor (e.g. a society or other partner) holds exclusive rights to this article under a publishing agreement with the author(s) or other rightsholder(s); author self-archiving of the accepted manuscript version of this article is solely governed by the terms of such publishing agreement and applicable law.

© The Author(s), under exclusive licence to Springer Nature Limited 2025

Methods

Detailed methods are included in the Supplementary Methods.

Reporting summary

Further information on research design is available in the Nature Portfolio Reporting Summary linked to this article.

Data availability

Metabolomics data are available at Zenodo (https://doi.org/10.5281/zenodo.15361205)[44]. Additional patient data that cannot be shared due to privacy reasons are located in controlled access storage at NYU Langone Health. Source data are provided with this paper. Code availability Code used to analyse Patch Clamp data is available at GitHub (https://github.com/songs05/IonLab/tree/Ephys-Analysis).

Code availability

Code used to analyse Patch Clamp data is available at GitHub (https://github.com/songs05/IonLab/tree/Ephys-Analysis).

44. Guangbin, S. et al. Metabolomics data for CoQ headgroup intermediate plasma concentrations and incorporation into CoQ. *Zenodo* https://doi.org/10.5281/zenodo.15361205 (2025).

Acknowledgements We thank the staff of the DART Microscopy Laboratory, A. Liang, J. Sall and J. Liang, for their consultation and assistance with TEM work; I. Diaz for help and statistical discussions in presenting the single-patient IND data; D. N. Stephen for sectioning early postnatal mouse brains; D. M. Sabatini, D. E. Biancur, G. Francis Jr, J. Rodencal, S. Feske and W. Coetzee for critical reading and comments on the paper; K. Astudillo for the assistance in implementing the IRB protocol; the NYU Metabolomics Core Resource Laboratory (RRID: SCR_017935), Rodent Behavioral Laboratory (RRID: SCR_017935), IonLab (RRID: SCR_021754), Experimental Pathology Laboratory and DART Microscopy Laboratory for their assistance in obtaining the data presented here; and the patient and his family as well as the reviewers at the Division of Neurology I, US Food and Drug Administration and the NYU IRB for their expeditious review of this treatment. These cores are partially supported by the Cancer Center Support Grant P30CA016087 at the Laura and Isaac Perlmutter Cancer Center. M.E.P. is a Damon Runyon-Rachleff Innovation awardee supported in part by the Damon Runyon Cancer Research Foundation (DRR 63-20) and is the recipient of a Pershing Square Sohn Prize for Young Investigators in Cancer Research and the MIND Prize from the Pershing Square Foundation, the Tara Miller Melanoma Foundation – MRA Young Investigator Award (668365), a Basic Research Grant from the Harry J. Lloyd Charitable Trust, an ACS Research Scholar Award (RSG-21-115-01-MM), an NIGMS R35 MIRA from the NIH (1R35GM147119), an Irma T. Hirschl Career Scientist Award, a Concern Foundation Conquer Cancer Now Grant, a Harrington Scholar–Innovator Award and an Oxford-Harrington Rare Disease Scholar Award and research funding from NYU Langone Health Technology Opportunities and Ventures. R.S.B. is a Damon Runyon Dale F. Frey awardee supported by the Damon Runyon Cancer Research Foundation (DRG-50-22) and the NCI (R37CA289040). A.L.J. is supported by grants from the NIH (R37MH085726 and R01NS092096) and by an NCI Cancer Center Support Grant (CCSG, P30 CA08748) and Cycle for Survival. S.E.N. was supported by a François Wallace Monahan Fellowship. R.V.S. was supported by R01NS119301, R01NS127435 and P50HD103555 (Cell and Tissue Pathogenesis Core of the BCM IDDRC). S.K. is supported by a fellowship of Takeda Science Foundation, a fellowship of Astellas Foundation for Research on Metabolic Disorders and a fellowship of Mochida Memorial Foundation for Medical and Pharmaceutical Research. The clinical portion of this research is supported in part by the NYU-H+H Clinical and Translational Science Institute (CTSI), which is supported by the National Center for Advancing Translational Sciences (NCATS), National Institutes of Health, through grant award number UL1TR001445. The NYU Metabolomics Core Resource Laboratory (RRID: SCR_017935) is partially supported by Cancer Center Support Grant P30CA016087 at the Laura and Isaac Perlmutter Cancer Center. Support for NYU Langone Health's Ion Laboratory (RRID: SCR_021754) is partially provided through the Office of Scientific Research, NIH R01 AI097302, NIH subaward D009105901, Sophion Industries and Nanion Technologies. Behavioural and continuous metabolic home-cage experiments were performed in the NYULMC Rodent Behavior Laboratory (RRID: SCR_017942) supported by the NIH BRAIN Initiative U19NS1076 (A.C.M.). Q37

Author contributions G.S., R.S.B. and M.E.P. conceived and planned the research. G.S., Q.S., M.K., S.K., Z.W., W.C.T., S.C.S., A.G.R.H., T.L. and S.E.N. designed and carried out experiments. A.G.R.H., T.L., R.V.S., S.E.N., A.L.J. and M.S. interpreted histology. M.K., L.F. and D.R.J. performed metabolomic analysis. B.G.L. and A.C.M. designed, conducted, analysed and interpreted the behavioural assays. S.C.S. carried out and S.C.S., A.G.R.H. and R.V.S. interpreted electrophysiological measurements. C.M. and G.M.R. wrote the single-patient IND and IRB protocol for treatment of the patient. C.M. and G.M.R. wrote the clinical-trial protocol, treated the patient, collected and analysed all single-patient data without input from the other authors. C.M. treated the patient and collected all single-patient data without input from the other authors. M.E.P. wrote and A.G.R.H., A.L.J., R.V.S., R.S.B. and M.E.P. edited the paper, except for the section on the treatment of the single patient, which C.M. and G.M.R. wrote and edited independently. All authors reviewed and approved the paper. Q38

Competing interests G.S., Q.S., R.S.B. and M.E.P. are co-inventors on patents related to the use of 4-HMA, 4-HB and analogues in the diagnosis and treatment of neurodevelopmental and other diseases assigned to New York University. M.E.P. directly supervised the preclinical research. The treatment was conducted and supervised by C.M. and G.M.R. under an institutional conflict-of-interest management plan designed and implemented by NYU Langone Health in accordance with its policies. M.E.P. consulted on the clinical protocol and C.M. and G.M.R. directed the course of treatment in accordance with the institutional plan. Financial support for the clinical treatment was provided by the Pershing Square Foundation. The other authors declare no competing interests. Q39

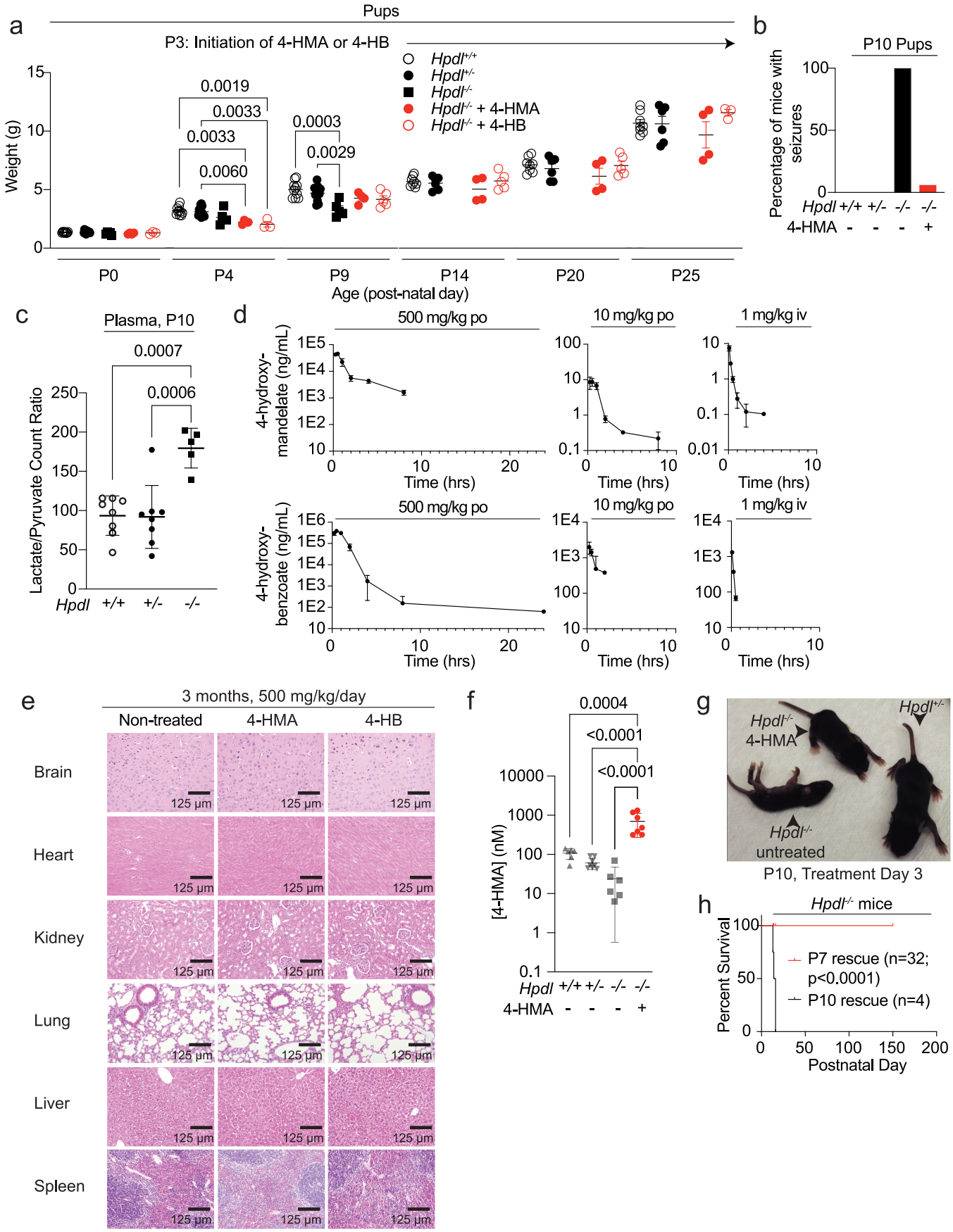
Additional information

Supplementary information The online version contains supplementary material available at https://doi.org/10.1038/s41586-025-09246-x. Q41

Correspondence and requests for materials should be addressed to Michael E. Pacold. Q42

Peer review information *Nature* thanks Jared Rutter and the other, anonymous, reviewer(s) for their contribution to the peer review of this work.

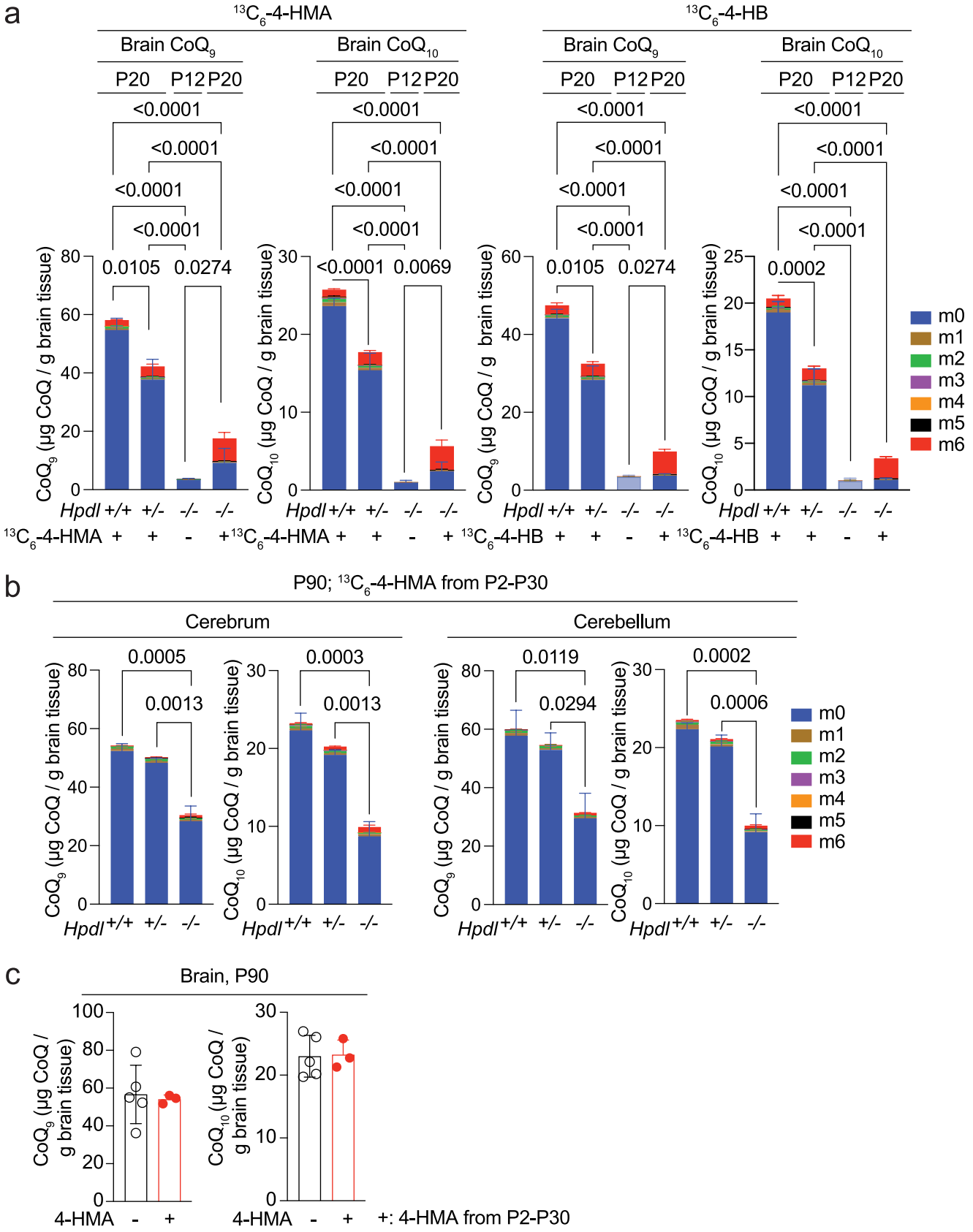
Reprints and permissions information is available at http://www.nature.com/reprints.



Extended Data Fig. 1 | See next page for caption.

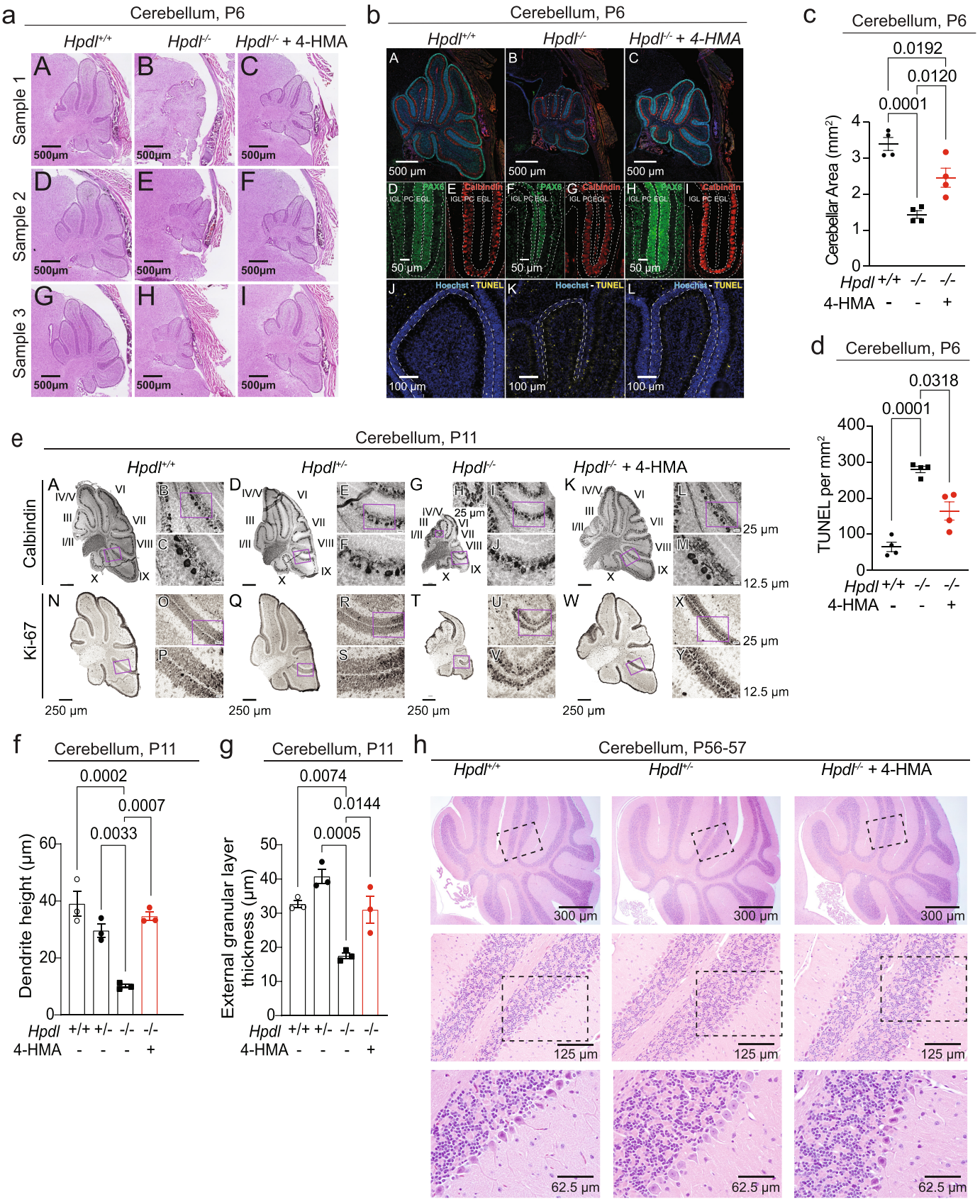
Extended Data Fig. 1 | related to Fig. 1, Mammalian CoQ headgroup intermediates improve the survival of *Hpdl*$^{-/-}$ mice and are incorporated into mouse brain CoQ$_9$ in vivo. a, *Hpdl*$^{-/-}$ pups (n = 5) exhibit significant weight loss by post-natal day 10 (P10) relative to *Hpdl*$^{+/+}$ (n = 8) and *Hpdl*$^{+/-}$ (n = 6) pups. Treatment of *Hpdl*$^{-/-}$ pups with 4-HMA (n = 4), the product of HPDL, and 4-HB (n = 5), the immediate precursor of the CoQ headgroup, results in weight gain similar to *Hpdl*$^{+/-}$ pups after P9. Error bars represent median±interquartile range. b, Seizure frequencies in pups. All *Hpdl*$^{-/-}$ pups (n = 6) have observed seizures. No *Hpdl*$^{+/+}$ (n = 6) or *Hpdl*$^{+/-}$ (n = 8) pups had observed seizures. Treatment with 4-HMA reduced the number of *Hpdl*$^{-/-}$ pups with seizures to 6 out of a total of 93 treated *Hpdl*$^{-/-}$ pups. c, Lactate/pyruvate ratio in plasma from *Hpdl*$^{+/+}$ (n = 8), *Hpdl*$^{+/-}$ (n = 8), and *Hpdl*$^{-/-}$ (n = 5) pups. *Hpdl*$^{-/-}$ pups have a higher lactate/pyruvate ratio than *Hpdl*$^{+/+}$ and *Hpdl*$^{+/-}$ pups. d, Pharmacokinetic data for 4-HMA and 4-HB at 500 mg/kg po and 1 mg/kg IV. Error bars represent mean ± standard deviation for data from 3 mice. e, Long-term toxicity histology for 4-HMA and 4-HB administered orally for 3 months at 500 mg/kg/day. No inflammation or necrosis were observed in the brain, heart, kidneys, liver, lungs, or spleen from untreated, 4-HMA, or 4-HB-treated mice. Sections are representative of n = 4 mice in each group. f, Plasma concentrations of 4-HMA in P10 *Hpdl*$^{-/-}$ pups treated with 10 mg/kg/day, orally administered 4-HMA starting at P3. Plasma 4-HMA concentrations are higher in treated *Hpdl*$^{-/-}$ pups than in *Hpdl*$^{+/+}$, *Hpdl*$^{+/-}$, and untreated *Hpdl*$^{-/-}$ pups. *Hpdl*$^{+/+}$, *Hpdl*$^{+/-}$, and *Hpdl*$^{-/-}$ pup data were obtained for Fig. 1c and are presented in a faded shade for ease of interpretation. 4-HMA-treated *Hpdl*$^{-/-}$ pup n = 7. g, *Hpdl*$^{-/-}$ pups can stand 3 days after supplementation with 4-HMA (10 mg/kg/day, oral administration). h, Survival of *Hpdl*$^{-/-}$ pups treated on P7 or P10. *Hpdl*$^{-/-}$ pups treated by postnatal day 7 (n = 32) survive into adulthood. Treatment of *Hpdl*$^{-/-}$ pups at 10 days after birth (n = 4) does not improve their survival. Significance was tested by two-way analysis of variance (ANOVA) followed by Tukey's post-hoc test.

Q40



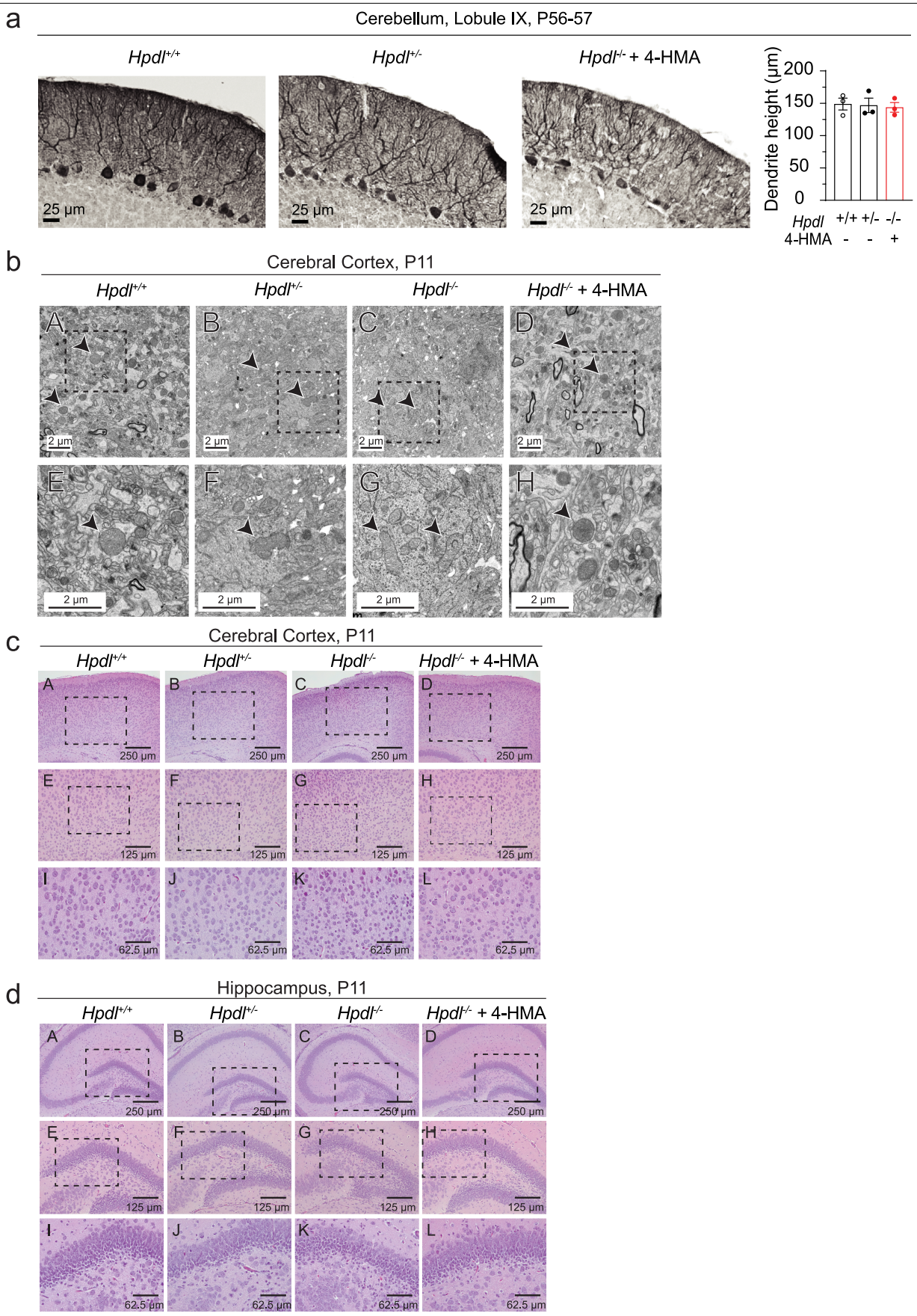
Extended Data Fig. 2 | See next page for caption.

Extended Data Fig. 2 | related to Fig. 1. CoQ concentrations in the brains of pups and P90 mice following 4-HMA and 4-HB treatment. a, CoQ_9 and CoQ_{10} concentrations from mouse brains following treatment with $^{13}C_6$-4-HMA or $^{13}C_6$-4-HB starting at postnatal day 3. $^{13}C_6$-4-HMA and $^{13}C_6$-4-HB are incorporated into CoQ_9 and CoQ_{10} in *Hpdl*$^{-/-}$ mice, and increase brain CoQ_9 relative to untreated *Hpdl*$^{-/-}$ mice. $^{13}C_6$-4-HMA and $^{13}C_6$-4-HB are minimally incorporated into CoQ_9 in *Hpdl*$^{+/+}$ mice and is incorporated into CoQ_9 at a lower fraction in *Hpdl*$^{+/-}$ mice. $^{13}C_6$-4-HMA: *Hpdl*$^{+/+}$ n = 3, *Hpdl*$^{+/-}$ n = 6, and *Hpdl*$^{-/-}$ treated n = 5. $^{13}C_6$-4-HB: *Hpdl*$^{+/+}$ n = 3, *Hpdl*$^{+/-}$ n = 4, and *Hpdl*$^{-/-}$ treated n = 3. *Hpdl*$^{-/-}$ untreated n = 3. CoQ_9 and CoQ_{10} data from *Hpdl*$^{-/-}$ untreated mice were obtained in the 4-HMA experiment and are presented in a faded shade of color in the 4-HB experiment for ease of interpretation. b, CoQ_9 and CoQ_{10} concentrations from the cortex and cerebellum of mice treated with $^{13}C_6$-4-HMA from P2-P30 and sacrificed at P90. The concentrations of CoQ_9 and CoQ_{10} in the brains of treated *Hpdl*$^{-/-}$ mice are ~50% of the concentrations of these molecules in the brains of *Hpdl*$^{+/+}$ mice. Only a minor fraction of CoQ_9 and CoQ_{10} is labeled with ^{13}C. *Hpdl*$^{+/+}$ n = 3, *Hpdl*$^{+/-}$ n = 3, and *Hpdl*$^{-/-}$ treated n = 3. c, CoQ_9 and CoQ_{10} concentrations from the brains of P90 wild-type mice that were not treated with 4-HMA, or treated with 4-HMA from P2-P30. 4-HMA does not increase the brain concentrations of CoQ_9 and CoQ_{10} in wild-type mice. Significance was tested by two-way analysis of variance (ANOVA) followed by Tukey's post-hoc test.



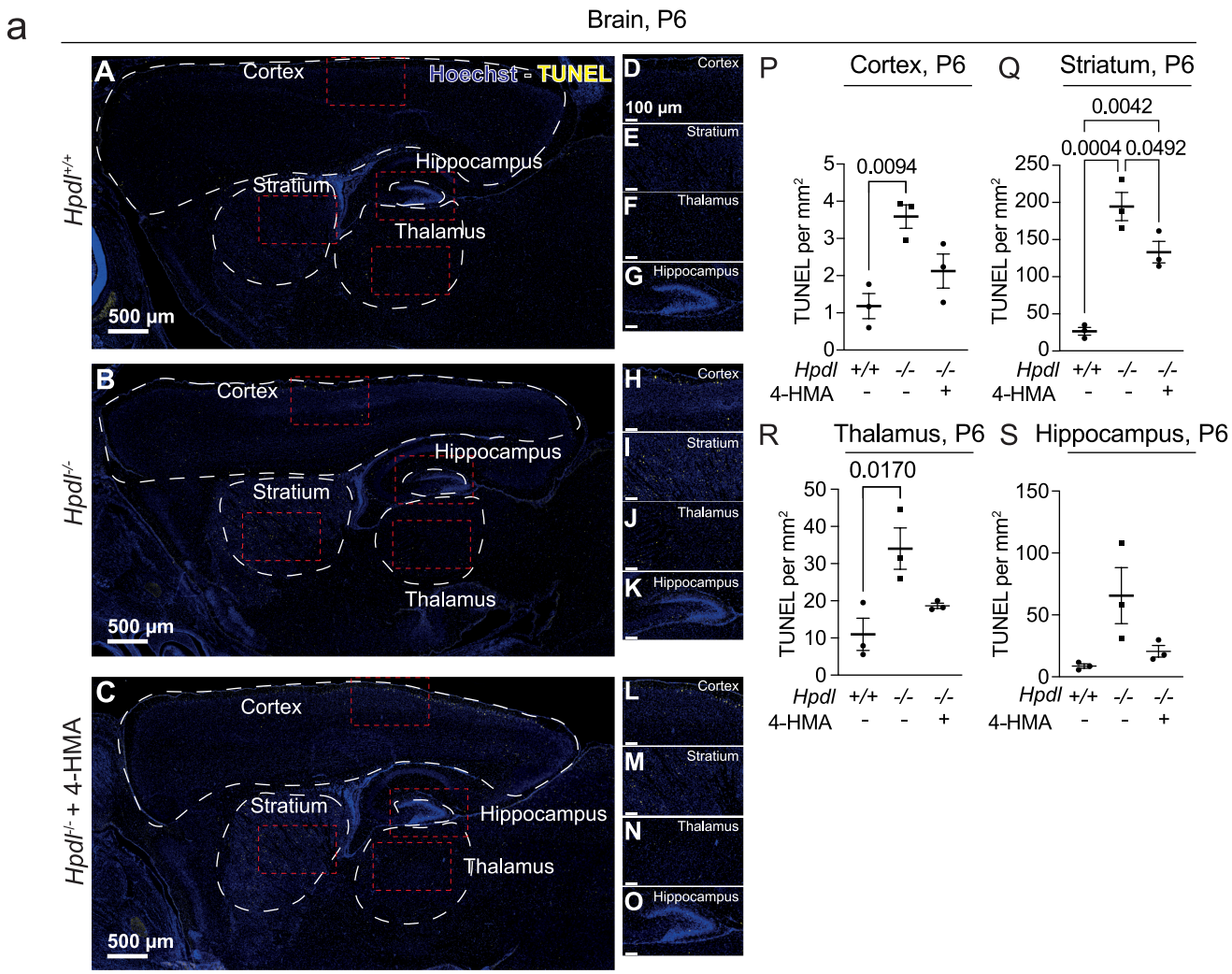
Extended Data Fig. 3 | See next page for caption.

Extended Data Fig. 3 | related to Fig. 2. 4-HMA supplementation improves the histologic appearances of the brains of *Hpdl*$^{-/-}$ mice. a, Hematoxylin and eosin staining of cerebellar samples from P6 *Hpdl*$^{+/+}$, *Hpdl*$^{-/-}$, and *Hpdl*$^{-/-}$ mice treated with 4-HMA (*Hpdl*$^{-/-}$ + *4-HMA*). Three *Hpdl*$^{+/+}$ (A, D and G), *Hpdl*$^{-/-}$ (B, E and H) and *Hpdl*$^{-/-}$ + 4-HMA (C, F and I) samples were analyzed to determine the reproducibility of the phenotype. *Hpdl*$^{-/-}$ mouse cerebella have pronounced atrophy that is partially rescued after 4-HMA treatment. b, Immunostaining for PAX6 (green) and Calbindin (red) on mid-sagittal sections of P6 cerebella from *Hpdl*$^{+/+}$, *Hpdl*$^{-/-}$, and *Hpdl*$^{-/-}$ mice treated with 4-HMA from P2-3 (*Hpdl*$^{-/-}$ + 4-HMA) (Panels A-C). Nuclei were counterstained with Hoechst (blue). Panels D-I are higher-magnification views of the boxed area in each image above with single-channel PAX6 (green) and Calbindin (red) staining. PAX6 stanning of granule cells shows that the EGL and IGL are depleted in the *Hpdl*$^{-/-}$ cerebella (Panel F compared to D, H). Calbindin staining of Purkinje cells shows the cells form a multilayer in *Hpdl*$^{-/-}$ cerebella (panel G). Purkinje cells form a single layer following 4-HMA treatment, but dendrites are stunted (panel I). Panels J-I contain lobule 3 from mid-sagittal cerebellar sections immunostained for Hoechst (blue) and TUNEL (yellow), showing an increase in cell death in *Hpdl*$^{-/-}$ cerebella (panel K) compared to control cerebella (panel J). 4-HMA treatment decreases cell death (Panel L). The white dashed line delineates the external granular layer of lobule 3. c, Quantitation of cerebellar area in midline sections from P6 pups in Extended Data Fig. 3b. *Hpdl*$^{-/-}$ pups have smaller cerebella than *Hpdl*$^{+/+}$ pups. Cerebellar size in *Hpdl*$^{-/-}$ pups is partially rescued by 4-HMA treatment. n = 4 for all groups. d, Quantitation of TUNEL staining, a measure of apoptosis, in the cerebella of P6 pups, from Extended Data Fig. 3b. *Hpdl*$^{-/-}$ pups have higher TUNEL staining in their cerebella than *Hpdl*$^{+/+}$ pups. TUNEL staining in *Hpdl*$^{-/-}$ pups is partially decreased by 4-HMA treatment, consistent with decreased levels of apoptosis when CoQ headgroup synthesis is restored. n = 4 for all groups. e, P11 *Hpdl*$^{-/-}$ pups show reduced Purkinje cell dendrite height (panels G-J) and EGL thickness (panels T-V) as revealed by calbindin antibody and Ki-67 antibody staining, respectively. P11 *Hpdl*$^{-/-}$ pups also demonstrate reduced cerebellar size (panel G) and ectopic Purkinje cells (panel H), indicative of abnormal Purkinje cell development. These abnormalities appear restored by 4-HMA treatment from P2-3 (panels K-M, W-Y). f, Quantitation of dendrite height shown in the calbindin stains from Extended Data Fig. 2e, which confirms that P11 *Hpdl*$^{-/-}$ pups have significantly reduced dendrite height that was rescued in the 4-HMA treated group. n = 3 animals per group. g, Quantitation of External Granular Layer (EGL) thickness shown in the Ki-67 stains from Extended Data Fig. 2e, which confirms that P11 *Hpdl*$^{-/-}$ pups have significantly reduced EGL thickness that was rescued in the 4-HMA treated group. n = 3 animals per group. h, Hematoxylin and eosin staining of cerebellar samples from P56-57 *Hpdl*$^{+/+}$, *Hpdl*$^{+/-}$, and *Hpdl*$^{-/-}$ mice treated with 4-HMA. The cerebellar histology is grossly normal in all three groups of animals. For panels c, d, f, and g, significance was tested by two-way analysis of variance (ANOVA) followed by Tukey's post-hoc test.

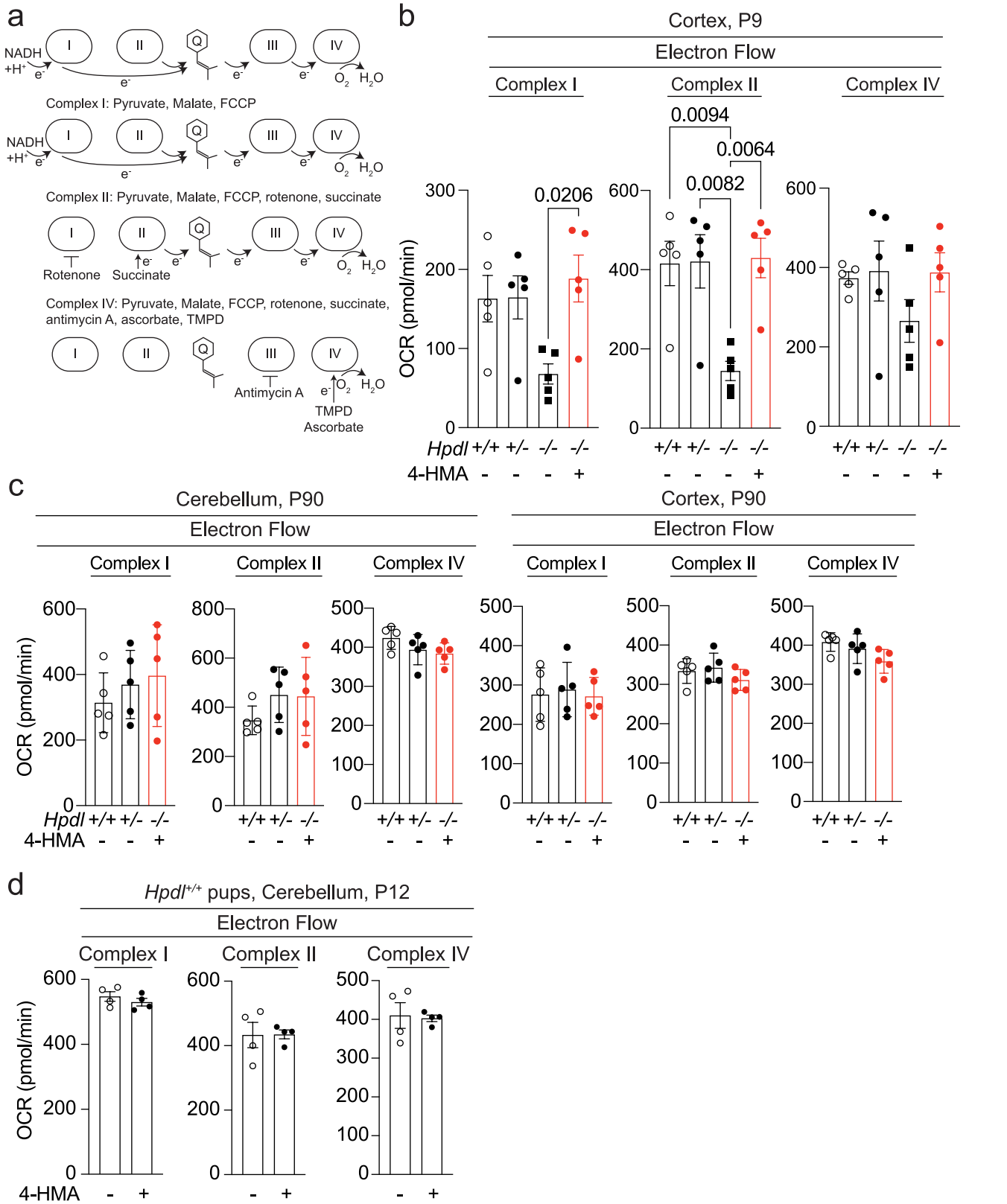


Extended Data Fig. 4 | See next page for caption.

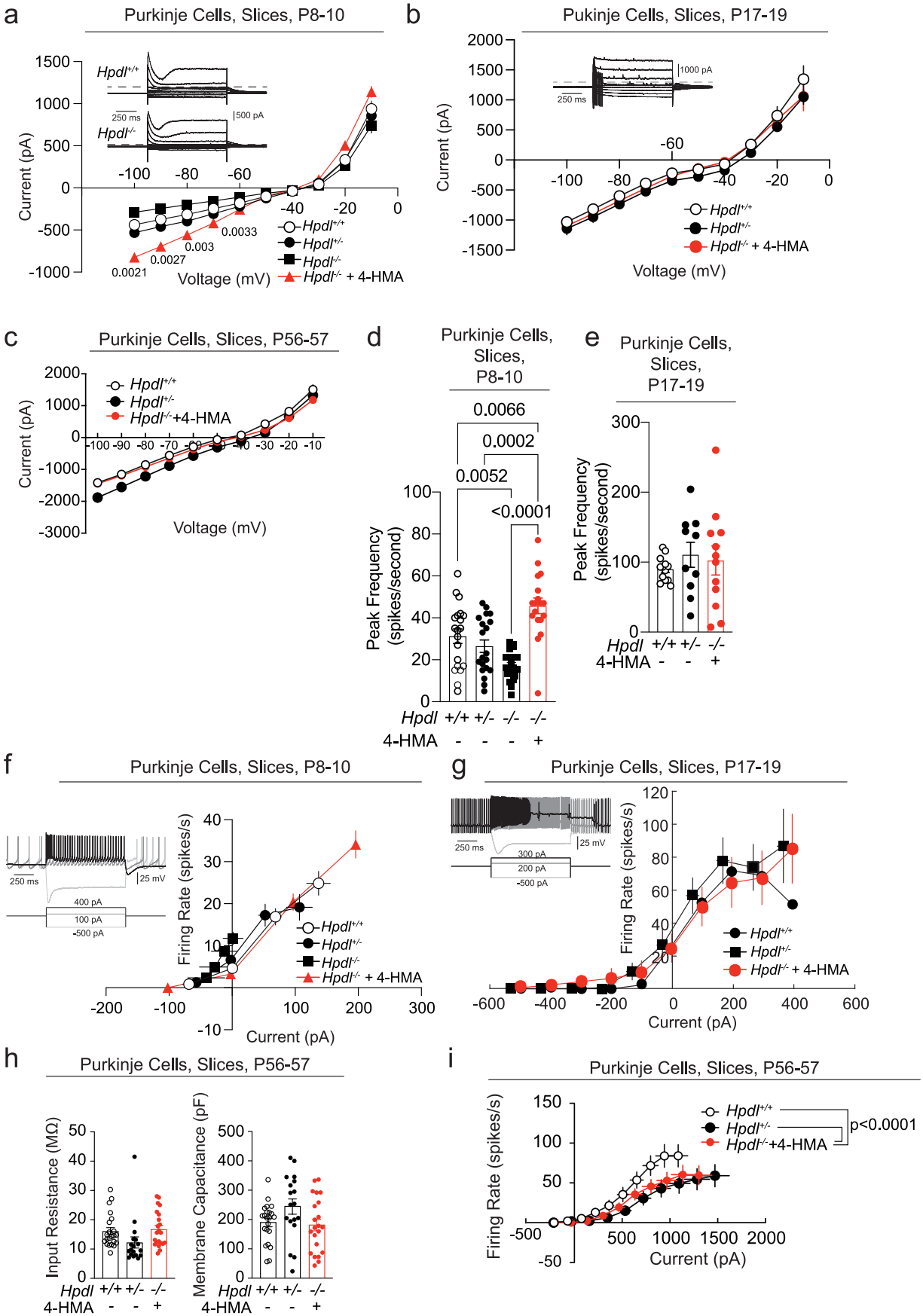
Extended Data Fig. 4 | related to Fig. 2. Additional histological characterization of untreated and 4-HMA-treated brains from *Hpdl*$^{-/-}$ mice. a, Representative calbindin staining of cerebellar sections from P56-57 *Hpdl*$^{+/+}$, *Hpdl*$^{+/-}$, and 4-HMA-treated *Hpdl*$^{-/-}$ mice and quantitation of dendrite height. The dendrite height is similar in all three groups of animals. b, Representative electron micrographs of the cortex in P11 *Hpdl*$^{+/+}$, *Hpdl*$^{+/-}$, and *Hpdl*$^{-/-}$ pups, as well as *Hpdl*$^{-/-}$ pups treated with 4-HMA. We observed minimal changes in cortical mitochondrial ultrastructure in *Hpdl*$^{-/-}$ pups (panels C and G) compared to *Hpdl*$^{+/+}$ pups (panels A and E) and *Hpdl*$^{+/-}$ pups (panels B and F). c, P11 *Hpdl*$^{-/-}$ pups exhibit subtle loss of normal cortical layers of the cerebral cortex (panels C, G, K), as well as edema, shrinking of the cortical neurons, and red neurons. These histological findings are partially restored by supplementation with 4-HMA (panels D, H, L). d, P11 *Hpdl*$^{-/-}$ pups do not exhibit major changes in hippocampal histology in comparison to *Hpdl*$^{+/+}$ pups, *Hpdl*$^{+/-}$ pups, and *Hpdl*$^{-/-}$ pups treated with 4-HMA. n = 4 for all groups. For panel a, significance was tested by two-way analysis of variance (ANOVA) followed by Tukey's post-hoc test.



Extended Data Fig. 5 | related to Fig. 2. TUNEL staining in the brains of untreated and 4-HMA-treated *Hpdl*$^{-/-}$ mice. a, Staining for Hoechst (blue) and TUNEL (yellow) showing the forebrain of *Hpdl*$^{+/+}$, *Hpdl*$^{-/-}$ and *Hpdl*$^{-/-}$ + 4-HMA mice at P6 (A-C). The white dashed lines delineate the approximate areas of the cortex, striatum, thalamus and hippocampus that were quantified. Magnified view of the red-boxed areas are on the right (D-O). n = 3 slides per mouse and 3 mice/genotype. The graphs represent the density of TUNEL+ particles per mm squared in the cortex (P), striatum (Q), thalamus (R) and hippocampus (S) of the *Hpdl*$^{+/+}$, *Hpdl*$^{-/-}$ and *Hpdl*$^{-/-}$ + 4-HMA mice at P6. For panels P-S, significance was tested by two-way analysis of variance (ANOVA) followed by Tukey's post-hoc test.

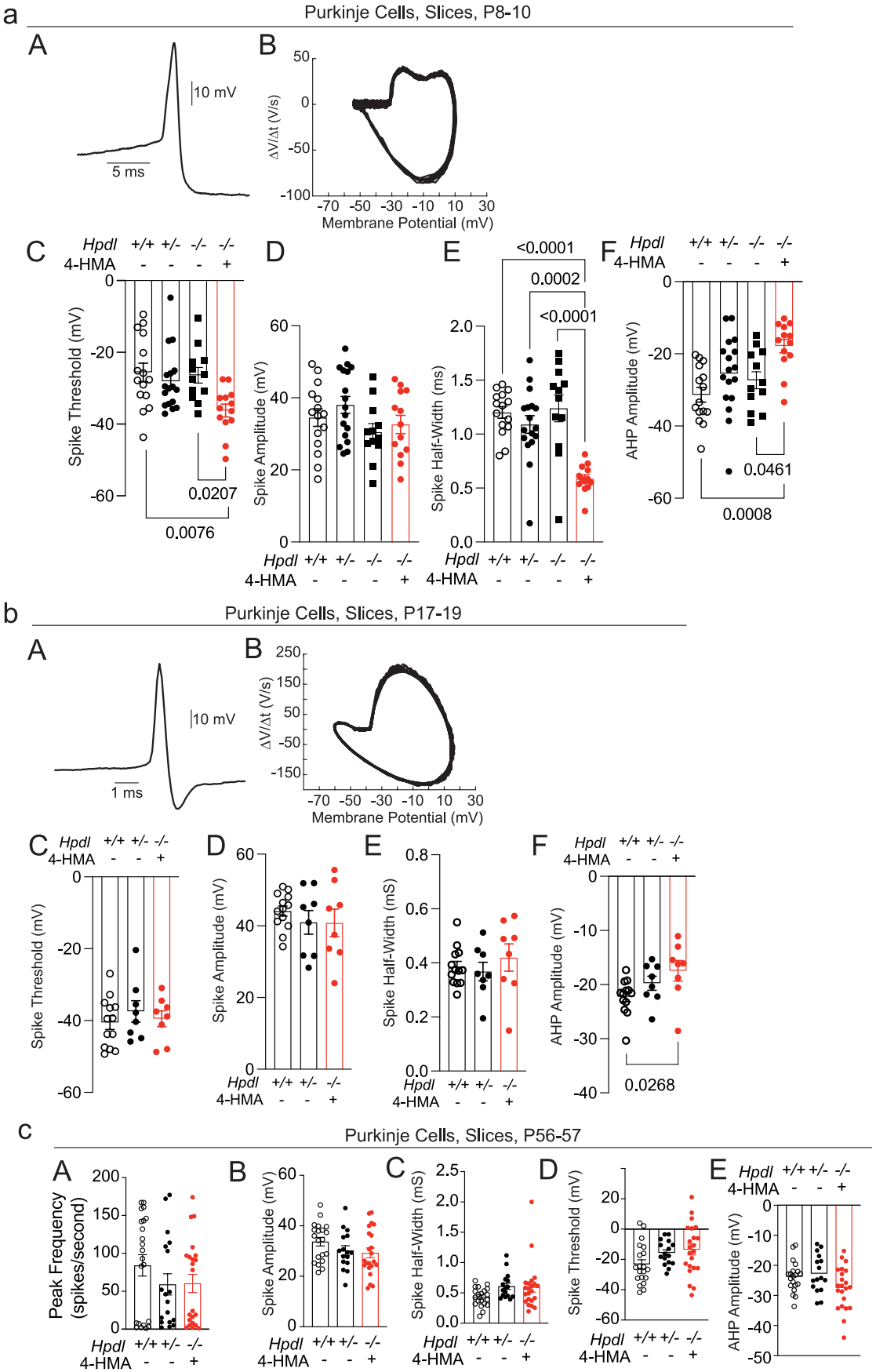


Extended Data Fig. 6 | related to Fig. 3. Electron flow measurements in cerebellum and co *Hpdl*$^{+/+}$, *Hpdl*$^{+/-}$, *Hpdl*$^{-/-}$ and 4-HMA-treated *Hpdl*$^{-/-}$ mice. a, Electron transport chain substrates and inhibitors used for the electron flow assay. I, Complex I. II, Complex II. III, Complex III. IV, Complex IV. Q, CoQ. b, Electron flow measurements of mitochondria isolated from the cortex of P9 *Hpdl*$^{+/+}$, *Hpdl*$^{+/-}$, and *Hpdl*$^{-/-}$ pups, as well as *Hpdl*$^{-/-}$ pups treated with 4-HMA. Electron flow through complex I and complex II is reduced in *Hpdl*$^{-/-}$ pups, and is improved by treatment with 4-HMA. c, Electron flow measurements of mitochondria isolated from the cortex and cerebellum of P90 (3-month-old) *Hpdl*$^{+/+}$ and *Hpdl*$^{+/-}$ pups, as well as *Hpdl*$^{-/-}$ pups treated with 4-HMA from P3-30. Electron flow through complexes I, II, and IV are similar in all groups. d, Electron flow measurements of mitochondria isolated from P12 *Hpdl*$^{+/+}$ mice treated with 4-HMA starting on P3. 4-HMA treatment does not increase electron flow through complex I, II, or IV in wild-type pups. Mitochondria were isolated from n = 5 animals for all groups. Significance was tested by two-way analysis of variance (ANOVA) followed by Tukey's post-hoc test.



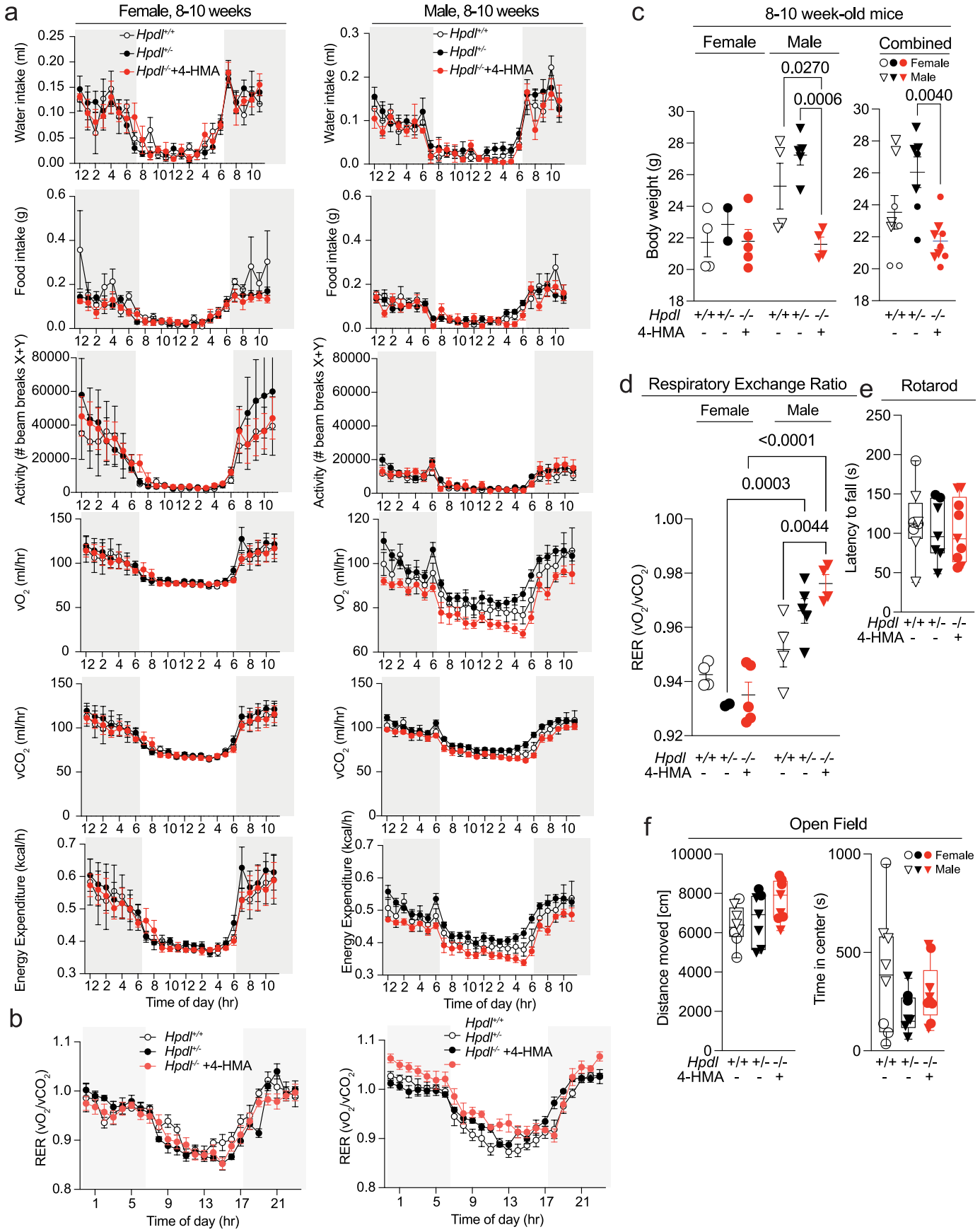
Extended Data Fig. 7 | See next page for caption.

Extended Data Fig. 7 | related to Fig. 3. Electrophysiologic characterization of Purkinje from *Hpdl*$^{+/+}$, *Hpdl*$^{+/-}$, *Hpdl*$^{-/-}$ and 4-HMA-treated *Hpdl*$^{-/-}$ mice. a, The I/V curves of Purkinje cells from P8-10 *Hpdl*$^{-/-}$ pups and 4-HMA-treated *Hpdl*$^{-/-}$ pups are significantly different from each other and from the I/V curves of *Hpdl*$^{+/+}$ and *Hpdl*$^{+/-}$ pups, which are similar. P-values indicating statistical significance are listed. The *Hpdl*$^{-/-}$ pups have a flatter I/V curve at hyperpolarized membrane potentials relative to the other curves due to a tighter grouping of currents at hyperpolarized membrane potentials (-100 to -60 mV) than the *Hpdl*$^{+/+}$ and *Hpdl*$^{+/-}$ pups (see insert). The 4-HMA-treated *Hpdl*$^{-/-}$ pups have a steeper I/V curve similar to more mature Purkinje cells. b. The I/V curves of Purkinje cells from P17-19 *Hpdl*$^{+/+}$, *Hpdl*$^{+/-}$, and 4-HMA-treated *Hpdl*$^{-/-}$ pups are similar. The inset depicts an example *Hpdl*$^{+/+}$ Purkinje cell current response to the voltage step commands, which is similar to the *Hpdl*$^{+/-}$ and 4-HMA-treated *Hpdl*$^{-/-}$ pup Purkinje cells responses. c, The I/V curves of Purkinje cells from P56-57 *Hpdl*$^{+/+}$, *Hpdl*$^{+/-}$, and 4-HMA-supplemented *Hpdl*$^{-/-}$ mice are comparable. d, Peak frequency of Purkinje cells from P8-10 *Hpdl*$^{+/+}$, *Hpdl*$^{+/-}$, *Hpdl*$^{-/-}$ and 4-HMA-treated *Hpdl*$^{-/-}$ pups. The 4-HMA treated *Hpdl*$^{-/-}$ group has higher peak frequency than any of the other groups. Differences in frequency were identified by two-way ANOVA followed by Dunnett's multiple comparison test. e, Peak frequency of Purkinje cells from P17-19 *Hpdl*$^{+/+}$, *Hpdl*$^{+/-}$, and 4-HMA-treated *Hpdl*$^{-/-}$ pups. The peak frequencies in all three groups are comparable. f, F/I curves of Purkinje cells from P8-10 *Hpdl*$^{+/+}$, *Hpdl*$^{+/-}$, *Hpdl*$^{-/-}$ and 4-HMA-treated *Hpdl*$^{-/-}$ pups. There were no significant differences in the linear portions of each curve between each group. The insert shows the simple firing pattern of an immature Purkinje cell. g, F/I curves of Purkinje cells from P17-19 *Hpdl*$^{+/+}$, *Hpdl*$^{+/-}$, *Hpdl*$^{-/-}$ and 4-HMA-treated *Hpdl*$^{-/-}$ pups. There were no significant differences in the linear portions of each curve between each group. The insert shows the simple firing pattern of a more mature Purkinje cell. h, Input resistance and membrane capacitance in Purkinje from P56-57 (8-week-old; age comparable to behavioral assays) *Hpdl*$^{+/+}$ and 4-HMA-supplemented *Hpdl*$^{-/-}$ mice are comparable, with a nonsignificant decrease in input resistance and a nonsignificant increase in membrane capacitance in *Hpdl*$^{+/-}$ mice and a nonsignificant increase in membrane capacitance. i, The F/I curve of Purkinje cells from P56-57 *Hpdl*$^{+/+}$ mice exhibits a higher firing rate at higher input currents than Purkinje cells from *Hpdl*$^{+/-}$ and 4-HMA-treated *Hpdl*$^{-/-}$ mice. All electrophysiological data are presented as the averages of at least 10 Purkinje cells (Supplementary Table 4). Significance was tested by two-way ANOVA followed by Tukey's post-hoc test.



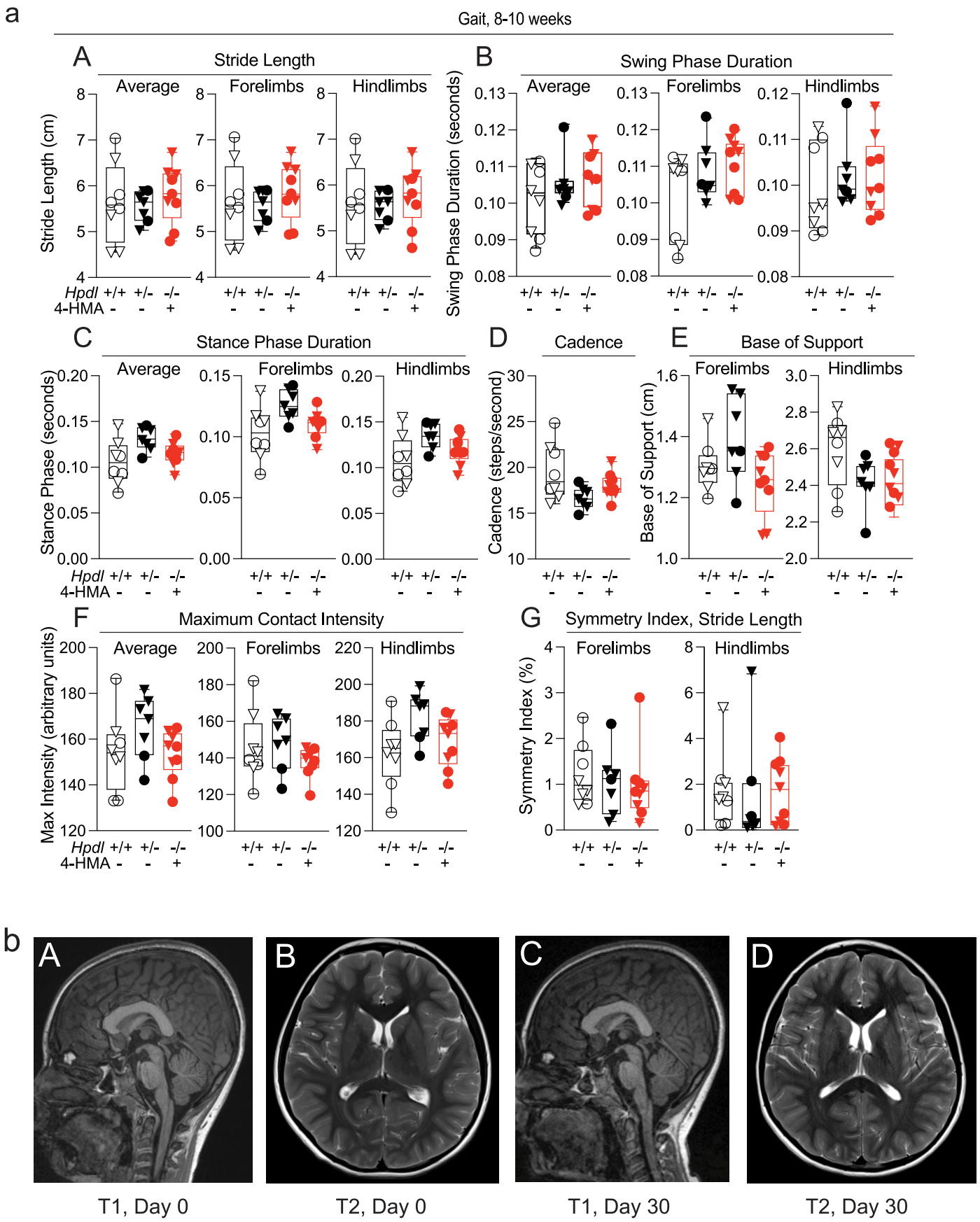
Extended Data Fig. 8 | See next page for caption.

Extended Data Fig. 8 | related to Fig. 3. Action potential characteristics of Purkinje cells from *Hpdl*$^{+/+}$, *Hpdl*$^{+/-}$, *Hpdl*$^{-/-}$ and 4-HMA-treated *Hpdl*$^{-/-}$ mice. a. Action potential characteristics of Purkinje cells from P8-10 *Hpdl*$^{+/+}$, *Hpdl*$^{+/-}$, *Hpdl*$^{-/-}$ and 4-HMA-treated *Hpdl*$^{-/-}$ pups. An average action potential is shown in panel A and the phase plane diagram is shown in panel B. Significant action potential shape differences can be seen between Purkinje cells from *Hpdl*$^{+/+}$ and 4-HMA-treated *Hpdl*$^{-/-}$ pups. Purkinje cells from 4-HMA-treated *Hpdl*$^{-/-}$ pups had a significantly lower spike threshold than the *Hpdl*$^{+/+}$ ($p = 0.0076$) and *Hpdl*$^{-/-}$ pups ($p = 0.0207$; panel C). The spike threshold for Purkinje cells from the *Hpdl*$^{+/-}$ and 4-HMA-treated *Hpdl*$^{-/-}$ pups trended to difference but was not significant ($p = 0.0506$), consistent with 4-HMA treatment rescuing *Hpdl*$^{-/-}$ pup grip strength to the level of *Hpdl*$^{+/-}$ mice (Fig. 3g). The spike half-width of Purkinje cells from the 4-HMA-treated *Hpdl*$^{-/-}$ pups was significantly narrower than all three treatments (*Hpdl*$^{+/+}$: $p < 0.0001$; *Hpdl*$^{+/-}$: $p = 0.0002$; *Hpdl*$^{-/-}$: $p < 0.0001$; panel E). Finally, Purkinje cells from 4-HMA-treated *Hpdl*$^{-/-}$ pups had a shallower action half-potential (AHP) amplitude compared to *Hpdl*$^{+/+}$ and *Hpdl*$^{-/-}$ pups (WT: $p = 0.0008$; KO: $p = 0.0461$; panel F). The 4-HMA-treated *Hpdl*$^{-/-}$ pup statistics resemble the WT condition of the P17-19 group (Extended Data Fig. 8b). b, Action potential characteristics of P17-19 *Hpdl*$^{+/+}$, *Hpdl*$^{+/-}$, and 4-HMA-treated *Hpdl*$^{-/-}$ pups. An average action potential is shown in panel A and the phase plane diagram is shown in panel B. The spike threshold, spike amplitude, and spike half-width are comparable in all three groups. The AHP for Purkinje cells from 4-HMA-treated *Hpdl*$^{-/-}$ pups was lower than for *Hpdl*$^{+/+}$ pups ($p = 0.0268$). c, Peak frequency and action potential characteristics of Purkinje cells from P56-57 *Hpdl*$^{+/+}$, *Hpdl*$^{+/-}$, and 4-HMA-treated *Hpdl*$^{-/-}$ mice. The peak frequency, spike amplitude, spike half-width, spike threshold, and AHP amplitude are comparable in all three groups. All electrophysiological data are presented as the averages of at least 10 Purkinje cells (Supplementary Table 4). Differences in frequency were identified by two-way ANOVA followed by Dunnett's multiple comparison test.



Extended Data Fig. 9 | See next page for caption.

Extended Data Fig. 9 | related to Fig. 3. Additional metabolic, behavioral, and neurological tests of *Hpdl*$^{+/+}$, *Hpdl*$^{+/-}$, *Hpdl*$^{-/-}$ and 4-HMA-treated *Hpdl*$^{-/-}$ mice. a, Metabolic phenotypes such as food and water intake, activity, O_2 consumption, CO_2 production, and energy expenditure are similar in 4-6-week-old *Hpdl*$^{+/+}$, *Hpdl*$^{+/-}$, and 4-HMA-treated *Hpdl*$^{-/-}$ mice, as measured in metabolic cages. There were no significant changes in any of these parameters between *Hpdl*$^{+/+}$, *Hpdl*$^{+/-}$, and 4-HMA-treated *Hpdl*$^{-/-}$ mice. b, Respiratory exchange ratio (vO_2/vCO_2) in *Hpdl*$^{+/+}$, *Hpdl*$^{+/-}$, and 4-HMA-treated *Hpdl*$^{-/-}$ mice. c, 4-HMA treatment partially restores the weight of male *Hpdl*$^{-/-}$ mice and rescues the weight of *Hpdl*$^{-/-}$ female mice. *Hpdl*$^{+/-}$ mice have comparable weights to *Hpdl*$^{+/+}$ mice. The combined data demonstrate that 4-HMA partially restores the weight of *Hpdl*$^{-/-}$ mice relative to *Hpdl*$^{+/-}$ mice. d, Respiratory exchange ratio summary in *Hpdl*$^{+/+}$, *Hpdl*$^{+/-}$, and 4-HMA-treated *Hpdl*$^{-/-}$ mice. Male *Hpdl*$^{-/-}$ mice treated with 4-HMA had a significantly increased respiratory exchange ratio (RER) compared to both *Hpdl*$^{+/+}$ male mice and *Hpdl*$^{+/-}$ and 4-HMA-treated *Hpdl*$^{-/-}$ female mice. e, Rotarod performance is similar in *Hpdl*$^{+/+}$, *Hpdl*$^{+/-}$, and 4-HMA-treated *Hpdl*$^{-/-}$ male and female mice. f, Open field data from 6–8-week-old *Hpdl*$^{+/+}$, *Hpdl*$^{+/-}$, and 4-HMA-treated *Hpdl*$^{-/-}$ mice revealed no significant differences in distance moved or time that mice spent in the center of the open field. Data from male mice are plotted as triangles. Data from female mice are plotted as circles. For behavioral tests, data from male mice (n: *Hpdl*$^{+/+}$ = 4, *Hpdl*$^{+/-}$ = 5, 4-HMA-treated *Hpdl*$^{-/-}$=4) are plotted as triangles. Data from female mice (n: *Hpdl*$^{+/+}$ = 4, *Hpdl*$^{+/-}$=2, 4-HMA-treated *Hpdl*$^{-/-}$=5) are plotted as circles. Behavioral data do not contain comparisons to untreated *Hpdl*$^{-/-}$ mice, which do not survive to the age at which these behavioral assays are carried out. Data presented are mean ± standard error of the mean, as well as raw data. Behavioral data are presented as box and whisker plots, where the center is the median, the box bounds are the 25th to 75th percentiles, and whiskers indicate minimum to maximum. Differences were identified by two-way ANOVA followed by Tukey's post-hoc test.



Extended Data Fig. 10 | See next page for caption.

Extended Data Fig. 10 | related to Figs. 3 and 4. Gait characterization of *Hpdl*$^{+/+}$, *Hpdl*$^{+/-}$, *Hpdl*$^{-/-}$ and 4-HMA-treated *Hpdl*$^{-/-}$ mice, and brain MRI from a patient with biallelic HPDL variants receiving the CoQ_{10} headgroup intermediate 4-HB. a, Additional catwalk data from 6–8-week-old *Hpdl*$^{+/+}$, *Hpdl*$^{+/-}$, and 4-HMA-treated *Hpdl*$^{-/-}$ mice reveal no significant differences in gait parameters between the groups of mice. A, stride length. B, swing phase duration. C, stance phase duration. D, cadence. E, base of support. F, maximum contact intensity. G, symmetry index for stride length. b, T1- and T2-weighted brain MRI images from a patient with biallelic *HPDL* variants before treatment with 4-HB (day 0; panels A and B) and 30 days after treatment with 4-HB (panels C and D). Data from male mice are plotted as triangles. Data from female mice are plotted as circles. For behavioral tests, data from male mice (n: *Hpdl*$^{+/+}$= 4, *Hpdl*$^{+/-}$= 5, 4-HMA-treated *Hpdl*$^{-/-}$=4) are plotted as triangles. Data from female mice (n: *Hpdl*$^{+/+}$= 4, *Hpdl*$^{+/-}$=2, 4-HMA-treated *Hpdl*$^{-/-}$=5) are plotted as circles. Behavioral data do not contain comparisons to untreated *Hpdl*$^{-/-}$ mice, which do not survive to the age at which these behavioral assays are carried out. Data presented are mean ± standard error of the mean, as well as raw data. Behavioral data are presented as box and whisker plots, where the center is the median, the box bounds are the 25th to 75th percentiles, and whiskers indicate minimum to maximum. Differences were identified by two-way ANOVA followed by Tukey's post-hoc test.

Author Queries

Journal: **Nature**
Paper: **s41586-025-09246-x**
Title: **Coenzyme Q headgroup intermediates can ameliorate a mitochondrial encephalopathy**

AUTHOR:
The following queries have arisen during the editing of your manuscript. Please answer by making the requisite corrections directly in the e.proofing tool rather than marking them up on the PDF. This will ensure that your corrections are incorporated accurately and that your paper is published as quickly as possible.

Query Reference	Reference
Q1	A single sentence summarizing your paper has been provided (editor's summary in the eproof), which will appear online on the table of contents and in e-alerts. Please check this sentence for accuracy and appropriate emphasis
Q2	For affiliations 6 and 7, we deleted 'Alexandria Center for Life Sciences West/East Tower' as per style. If the centre is part of the affiliation rather than a street address, please include it as part of the 'department'.
Q3	Please note we have amended the title for clarity.
Q4	Please check your article carefully, coordinate with any co-authors and enter all final edits clearly in the eproof, remembering to save frequently. Once corrections are submitted, we cannot routinely make further changes to the article.
Q5	Note that the eproof should be amended in only one browser window at any one time; otherwise changes will be overwritten.
Q6	Author surnames have been highlighted. Please check these carefully and adjust if the first name or surname is marked up incorrectly, as this will affect indexing of your article in public repositories such as PubMed. Also, carefully check the spelling and numbering of all author names and affiliations, and the corresponding author(s) email address(es). Please note that email addresses should only be included for designated corresponding authors, and you cannot change corresponding authors at this stage except to correct errors made during typesetting.
Q7	You cannot alter accepted Supplementary Information files except for critical changes to scientific content. If you do resupply any files, please also provide a brief (but complete) list of changes. If these are not considered scientific changes, any altered Supplementary files will not be used, only the originally accepted version will be published.

Author Queries

Journal: **Nature**
Paper: **s41586-025-09246-x**
Title:**Coenzyme Q headgroup intermediates can ameliorate a mitochondrial encephalopathy**

AUTHOR:
The following queries have arisen during the editing of your manuscript. Please answer by making the requisite corrections directly in the e.proofing tool rather than marking them up on the PDF. This will ensure that your corrections are incorporated accurately and that your paper is published as quickly as possible.

Query Reference	Reference
Q8	If applicable, please ensure that any accession codes and datasets whose DOIs or other identifiers are mentioned in the paper are scheduled for public release as soon as possible, we recommend within a few days of submitting your proof, and update the database record with publication details from this article once available.
Q9	Your paper has been copy edited. (1) Please review every sentence to ensure that it conveys your intended meaning; if changes are required, please provide further clarification rather than reverting to the original text. Please note that formatting (including hyphenation, Latin words, and any reference citations that might be mistaken for exponents) and usage have been made consistent with our house style.(2) Check the title and the first paragraph with care, as they may have been re-written to aid accessibility for non-specialist readers.(3) Check the symbols for affiliations with care, and check all author names and Acknowledgements carefully to ensure that they are correct; check the email address of the corresponding author and the Competing Interests statement.(4) Check that there has been no corruption of mathematical symbols. Only single-letter variables are set in italics (but not their subscripts unless these are also variables); multi-letter variables are set in roman. Vectors are set as bold; matrices are set as italic only. We do not use italics for emphasis. Genetic material is set in italic and gene products are set upright. Please check that italicization and bolding are correct throughout. (5) Ensure that, where practicable, all figures, tables and other discrete elements of Supplementary Information are referred to at least once in the paper at an appropriate place in the text or figure legends.(6) Please note, we reserve 'significant' and its derivatives for statistical significance. Please reword where this is not the intended meaning (for example, to important, notable, substantial).
Q10	Please check that the display items are as follows (ms no: 2024-04-08462): Figs 1-4; Tables: 1-4; Boxes: None; Extended Data display items: 1-10; SI (including reporting summary or peer review file): yes. The eproof contains the main-text figures edited by us and (if present) the Extended Data items (unedited except for minor formatting) and the Supplementary Information (unedited). Please check the edits to all main-text figures (and tables, if any) very carefully, and ensure that any error bars in the figures are defined in the figure legends. Extended Data items may be revised only if there are errors in the

Author Queries

Journal: **Nature**
Paper: **s41586-025-09246-x**
Title: **Coenzyme Q headgroup intermediates can ameliorate a mitochondrial encephalopathy**

AUTHOR:
The following queries have arisen during the editing of your manuscript. Please answer by making the requisite corrections directly in the e.proofing tool rather than marking them up on the PDF. This will ensure that your corrections are incorporated accurately and that your paper is published as quickly as possible.

Query Reference	Reference
	original submissions. If you need to revise any Extended Data items please upload these files when you submit your corrections to this eproof, and include a list of what has been changed.
Q11	Please ensure that genes are correctly distinguished from gene products: for genes, official gene symbols (e.g., NCBI Gene) for the relevant species should be used and italicized; gene products such as proteins and noncoding RNAs should not be italicized.
Q12	It is unclear what 'etc' means in Fig. 1a, is it OK to just have CoQ2 or do you mean 'CoQ2 and other co-enzymes'. Also COQ2 was changed to CoQ2, is this correct?
Q13	In Fig. 1e, should the bracketed part in the structure have a subscript n?
Q14	In Fig. 1a, please can you provide a definition for TAT?
Q15	(1) Please ensure that the following information is included in the figure legends where relevant. Sample size (exact n number); a statement of replicability (how many times was experiment replicated in the lab); description of sample collection (clarify whether technical or biological replicates and include how many animals, litters, cultures, etc.); state the statistical test used and give P values; define centre values (median or average) and error bars. (2) For figures/images that are reproduced or adapted from a third party, it is important that you confirm that permission has been obtained and that appropriate acknowledgement of the copyright holder is given. (3) Please note that we edit the main figures (but not the Extended Data figures) in house. There is no need to resupply any of the main figures to make minor changes to text labels to match the changes made in the text, as figures will have been edited accordingly. If you wish to make changes to any Extended Data figures, however, please resupply these, and please let us know what has changed.

Author Queries

Journal: **Nature**
Paper: **s41586-025-09246-x**
Title:**Coenzyme Q headgroup intermediates can ameliorate a mitochondrial encephalopathy**

AUTHOR:
The following queries have arisen during the editing of your manuscript. Please answer by making the requisite corrections directly in the e.proofing tool rather than marking them up on the PDF. This will ensure that your corrections are incorporated accurately and that your paper is published as quickly as possible.

Query Reference	Reference
Q16	Please can you confirm if the sentence ending '...would result in 13C6-CoQ9 and 13C6-CoQ10 (m6-CoQ9 and m6-CoQ10; Fig. 1e).' has been reworded correctly?
Q17	In Fig. 2a and c, please explain what the dashed boxes shows?
Q18	In Fig. 2b caption, where is reads '677 (Hpdl−/)' we changed this to 677 (Hpdl−/−), please confirm if this is correct?
Q19	Please check the panels and caption of Fig. 2 carefully, as these have been edited for style and clarity. Please make sure that any abbreviations listed only in the figure are defined in the caption.
Q20	Since the references were not cited in numerical order, they have been renumbered in the order of appearance. Please check.
Q21	In Fig. 3a, please can you define OCR?
Q22	In the graphic of Fig. 3b, we have added '200' on to the y axis, please confirm if this has been done correctly?
Q23	Please check the panels and caption of Fig. 3 carefully, as these have been edited for style and clarity. Please make sure that any abbreviations listed only in the figure are defined in the caption.
Q24	It is our style to set vectors upright and boldface. We set scalar variables italic, but not their subscripts (unless the subscripts are themselves variables; letters that are labels, such as 'i' for 'initial', are set upright). We set capital Greek letters in italics if they are variables. We set i, Euler's number (e) and pi upright. Please check that the maths has been formatted correctly according to this style.

Author Queries

Journal: **Nature**
Paper: **s41586-025-09246-x**
Title: **Coenzyme Q headgroup intermediates can ameliorate a mitochondrial encephalopathy**

AUTHOR:
The following queries have arisen during the editing of your manuscript. Please answer by making the requisite corrections directly in the e.proofing tool rather than marking them up on the PDF. This will ensure that your corrections are incorporated accurately and that your paper is published as quickly as possible.

Query Reference	Reference
Q25	As tables should be able to be understood as standalone items, we have included an explanation for –, please confirm if this is correct?
Q26	Reference [40] is a duplicate of [20] and hence the repeated version has been deleted. Please check.
Q27	Please can you confirm that the sentence 'A gene-dosage effect was observed in forelimb grip strength, with significant reductions found in 4-HMA-treated Hpdl−/− mice relative to Hpdl+/− and Hpdl+/+ mice ($F_{2,17} = 38.908$, $P < 0.001$), and with Hpdl+/− mice having significantly lower forelimb grip strength than Hpdl+/+ mice (Fig. 3g).' has been reworded correctly?
Q28	Please can you confirm if the sentences 'This pattern was similar but less pronounced in measures averaging grip strength for all four limbs. Only Hpdl−/− mice treated with 4-HMA had significant reductions in grip strength relative to Hpdl+/+ mice ($F_{2,17} = 4.358$, $P < 0.05$; Fig 3g).' have been reworded correctly?
Q29	Here is states '...two younger siblings who had died in infancy...' but in the caption for Fig. 4 it states older, please confirm which is correct?
Q30	Please can you confirm that VCV001344855.5 and VCV002221909.2 are linked correctly? One seems to be referring to an outdated entry.
Q31	Please check the panels and caption of Fig. 4 carefully, as these have been edited for style and clarity. Please make sure that any abbreviations listed only in the figure are defined in the caption.
Q32	Please note, we reserve 'significant' and its derivatives for statistical significance. Please reword where this is not the intended meaning (for example, relevance).

Author Queries

Journal: **Nature**
Paper: **s41586-025-09246-x**
Title:**Coenzyme Q headgroup intermediates can ameliorate a mitochondrial encephalopathy**

AUTHOR:
The following queries have arisen during the editing of your manuscript. Please answer by making the requisite corrections directly in the e.proofing tool rather than marking them up on the PDF. This will ensure that your corrections are incorporated accurately and that your paper is published as quickly as possible.

Query Reference	Reference
Q33	In Table 3, please can you define NA (is 'not applicable' or 'not available')?
Q34	Please can you confirm whether 'Although 4-HMA treatment improves most neurological deficits and improves the survival of Hpdl−/− mice when administered by day 6 or 7 postnatally…' has been reworded correctly?
Q35	In the sentence that starts 'Treatment with 13C6-4-HMA or 4-HB restores CoQ9 and CoQ10 pools in Hpdl−/− mice…' should 4-HB also start with 13C6 (so 13C6-4-HB)?
Q36	CE: We have deleted references (47- 57) from refernce list and added in esm file. Please check.
Q37	(1) The acknowledgments have been edited for style and brevity; note, we do not include titles or affiliations and only include the initial(s) of the first name(s) of colleagues mentioned here. Please check. (2) Please check that all funders have been appropriately acknowledged and that all grant numbers are correct.
Q38	Please note that in the Acknowledgements and Author contributions sections we have updated some of the author initials to match the author list, please confirm if they have been amended correctly: S.S. to S.C.S., A.R.H. to A.G.R.H., S.E. to S.E.N., R.S. to R.V.S. and G.R. to G.M.R.
Q39	Please check that the Competing Interests declaration is correct as stated. If you declare competing interests, please check the full text of the declaration for accuracy and completeness.
Q40	Please check the Extended Data figure titles. Please make sure these are a descriptive title for each figure, and please move any other information to the caption as needed.

Author Queries

Journal: **Nature**
Paper: **s41586-025-09246-x**
Title: **Coenzyme Q headgroup intermediates can ameliorate a mitochondrial encephalopathy**

AUTHOR:
The following queries have arisen during the editing of your manuscript. Please answer by making the requisite corrections directly in the e.proofing tool rather than marking them up on the PDF. This will ensure that your corrections are incorporated accurately and that your paper is published as quickly as possible.

Query Reference	Reference
Q41	We have written p.o. and i.v. as orally and intravenously throughout, please check and confirm if this is correct?
Q42	Can you confirm this is correct, we say two -/- are on the left, and two +/- are on the right, so second from the right would be a +/- correct?
Q43	As refs. 46–57 are only cited in the Supplementary Information, the references were removed from the reference list in the main article and included in the Supplementary Information (s1) instead. Please check and confirm the references are cited correctly in the Supplementary Information.

nature portfolio

Corresponding author(s): Michael Pacold

Last updated by author(s): May 9, 2025

Reporting Summary

Nature Portfolio wishes to improve the reproducibility of the work that we publish. This form provides structure for consistency and transparency in reporting. For further information on Nature Portfolio policies, see our Editorial Policies and the Editorial Policy Checklist.

Statistics

For all statistical analyses, confirm that the following items are present in the figure legend, table legend, main text, or Methods section.

n/a	Confirmed
☐	☒ The exact sample size (*n*) for each experimental group/condition, given as a discrete number and unit of measurement
☐	☒ A statement on whether measurements were taken from distinct samples or whether the same sample was measured repeatedly
☐	☒ The statistical test(s) used AND whether they are one- or two-sided *Only common tests should be described solely by name; describe more complex techniques in the Methods section.*
☐	☒ A description of all covariates tested
☐	☒ A description of any assumptions or corrections, such as tests of normality and adjustment for multiple comparisons
☐	☒ A full description of the statistical parameters including central tendency (e.g. means) or other basic estimates (e.g. regression coefficient) AND variation (e.g. standard deviation) or associated estimates of uncertainty (e.g. confidence intervals)
☐	☒ For null hypothesis testing, the test statistic (e.g. *F*, *t*, *r*) with confidence intervals, effect sizes, degrees of freedom and *P* value noted *Give P values as exact values whenever suitable.*
☒	☐ For Bayesian analysis, information on the choice of priors and Markov chain Monte Carlo settings
☒	☐ For hierarchical and complex designs, identification of the appropriate level for tests and full reporting of outcomes
☒	☐ Estimates of effect sizes (e.g. Cohen's *d*, Pearson's *r*), indicating how they were calculated

Our web collection on statistics for biologists contains articles on many of the points above.

Software and code

Policy information about availability of computer code

Data collection	Metabolic home cage data were acquired and exported with TSE PhenoMaster software 8.1.4.14156. Patch-clamp recordings were collected with Clampex 11 (Molecular Devices).
Data analysis	Mass spectrometry data were analyzed with Xcalibur 4.0.27.19 (ThermoFisher). Whole mount micrographs were stitched together with Adobe Photoshop 26.4.1 and cropped in Adobe Illustrator 29.3. Data were analyzed with GraphPad Prism 10.4.2. Patch clamp recordings were analyzed using custom written code in MATLAB R2024b (Mathworks). The code is available at GitHub: https://github.com/songs05/IonLab/tree/Ephys-Analysis.

For manuscripts utilizing custom algorithms or software that are central to the research but not yet described in published literature, software must be made available to editors and reviewers. We strongly encourage code deposition in a community repository (e.g. GitHub). See the Nature Portfolio guidelines for submitting code & software for further information.

Data

Policy information about availability of data

All manuscripts must include a data availability statement. This statement should provide the following information, where applicable:

- Accession codes, unique identifiers, or web links for publicly available datasets
- A description of any restrictions on data availability
- For clinical datasets or third party data, please ensure that the statement adheres to our policy

All data supporting the findings of this study are available within the paper and its Supplementary Information. Additional patient data cannot be shared due to reasons of privacy are located in controlled access storage at NYU Langone Health.Requests to access these data from qualified researchers trained in human subject confidentiality protocols may be sent to the NYU Langone Health Clinical and Translational Science Institute at CTSI@NYULangone.org. Data availability requires consent of the IND investigators (Dr. Claire Miller and Dr. Giulietta Riboldi), the NYU IRB, the patient, and family

Research involving human participants, their data, or biological material

Policy information about studies with human participants or human data. See also policy information about sex, gender (identity/presentation), and sexual orientation and race, ethnicity and racism.

Reporting on sex and gender	We carried out a single patient study with a male patient. Sex is reported in the manuscript.
Reporting on race, ethnicity, or other socially relevant groupings	Reporting on race, ethnicity, or other socially relevant groupings are not provided for this patient for privacy concerns.
Population characteristics	Single patient, 8 years of age, male, with biallelic HPDL variants (c.3G>C (p.Met1Ile), c.789delG (p.P264Lfs*51).
Recruitment	The patient was referred to the investigators by Dr. Joseph Gleeson at UCSD. Recuritment is biased by the rareness of the disease (~200 patients in the USA).
Ethics oversight	The administration of 4-HB was approved by the FDA (single patient IND # 170119) and the treatment protocol was approved by the NYU Institutional Review Board (protocol #s23-01512).

Note that full information on the approval of the study protocol must also be provided in the manuscript.

Field-specific reporting

Please select the one below that is the best fit for your research. If you are not sure, read the appropriate sections before making your selection.

☒ Life sciences ☐ Behavioural & social sciences ☐ Ecological, evolutionary & environmental sciences

For a reference copy of the document with all sections, see nature.com/documents/nr-reporting-summary-flat.pdf

Life sciences study design

All studies must disclose on these points even when the disclosure is negative.

Sample size	We used a minimum of n=3 for in vitro experiments based on prior data (Banh et al., Nature 20201; https://pubmed.ncbi.nlm.nih.gov/34471290/). We used a minimum of 5 mice (with the exception of P90 CoQ measurements, which used 3 mice due to prior knowledge of brain CoQ measurement robustness) for all in vivo experiments. Both in vitro and in vivo sample size were observed to yield appropriate statistical power.
Data exclusions	We did not exclude data from the analyses, except in occasional instances when an individual LC-MS run had poor signal or inadequate internal standard measurements.
Replication	All experiments were replicated a minimum of three times with independent biological samples.
Randomization	Initial mouse experiments were randomized 1:1 to treatment or vehicle. Following observation of treatment effects, additional mice were treated without randomization to determine the robustness of the treatment effect. All other data were acquired identically (within each experiment) using internally controls and did not require randomization.
Blinding	Blinding was not possible for in vivo mouse studies due to the the large differences in phenotype between treated and untreated animals. Blinding was not possible for the clinical portion of this work as only a single patient was treated. However, the corresponding author was blinded to the outcome of the single-patient clinical trial until 30 days of treatment.

Reporting for specific materials, systems and methods

We require information from authors about some types of materials, experimental systems and methods used in many studies. Here, indicate whether each material, system or method listed is relevant to your study. If you are not sure if a list item applies to your research, read the appropriate section before selecting a response.

Materials & experimental systems

n/a	Involved in the study
☐	☒ Antibodies
☒	☐ Eukaryotic cell lines
☒	☐ Palaeontology and archaeology
☐	☒ Animals and other organisms
☐	☒ Clinical data
☒	☐ Dual use research of concern
☒	☐ Plants

Methods

n/a	Involved in the study
☒	☐ ChIP-seq
☒	☐ Flow cytometry
☐	☒ MRI-based neuroimaging

Antibodies

Antibodies used

Calbindin (swant # 300; CB300PUR)
Ki-67 (BD Pharmingen #55069)
Pax6 (Millipore #AB2237)
HRP-conjugated goat anti-mouse secondary (Agilent DAKO #P044701-5)
HRP-conjugated goat anti-rabbit secondary (Agilent DAKO #P044801-2)
Alexa Fluor 488 donkey anti-rabbit (Invitrogen #A21206)
Alexa Fluor 555 donkey anti-mouse (Invitrogen #A31570)

Validation

Validation statements are available on the companies' websites as follows:
Calbindin: https://webshop.swant.com/affinity-purified-mouse-monoclonal-anti-calbindin-d-28k-100ul.html
Ki-67: https://www.bdbiosciences.com/en-us/products/reagents/flow-cytometry-reagents/research-reagents/single-color-antibodies-ruo/purified-mouse-anti-ki-67.550609
Pax6: https://www.emdmillipore.com/US/en/product/Anti-PAX6-Antibody,MM_NF-AB2237

Animals and other research organisms

Policy information about studies involving animals; ARRIVE guidelines recommended for reporting animal research, and Sex and Gender in Research

Laboratory animals	Mice (Mus musculus, C57BL/6NCrl-Hpdlem1(IMPC)Mbp/Mmucd; MMRRC:0066979-UCD; MGI 2444646) , aged 1-600 days
Wild animals	No wild animals were used in this research.
Reporting on sex	Sex was treated as a biological variable in these experiments. Sex was determined by measurement of anogenital distance. Behavioral data are disaggregated by sex.
Field-collected samples	No field-collected samples were used in this research.
Ethics oversight	All animal studies were approved by the NYULMC IACUC (Institutional Animal Care and Use Committee) under protocol IA16-01862 and conducted in accordance with IACUC guidelines and in observance of humane endpoints.

Note that full information on the approval of the study protocol must also be provided in the manuscript.

Clinical data

Policy information about clinical studies

All manuscripts should comply with the ICMJE guidelines for publication of clinical research and a completed CONSORT checklist must be included with all submissions.

Clinical trial registration	This study describes a single-patient IND that did not require registration as it is limited to a specific patient.
Study protocol	The protocol for this single patient IND is not available as it contains HIPAA-protected information.
Data collection	Data were collected over a period of 30 days, during the period of initial treatment, at the NYU Clinical and Translational Sciences Institute, located at Bellevue Hospital, New York, NY. Subsequent data collection was obtained at the NYU CTSI at 30 and 54 days following initiation of treatment. All treatment was conducted as an outpatient. From Day 30 to Day 54, the patient returned home.
Outcomes	Primary outcomes were the Modified Ashworth Scale (https://pubmed.ncbi.nlm.nih.gov/28901119/), Spastic Paraplegia Rating scale (https://pubmed.ncbi.nlm.nih.gov/16894103/), 9-hole Peg Test (https://pubmed.ncbi.nlm.nih.gov/25449717/) and 10-meter timed walk (https://pubmed.ncbi.nlm.nih.gov/32884845/), all of which are picked because they are established, validated measures of

spasticity. Each clinical datapoint was measured by the same physician throughout the study. Patient-reported outcomes were gathered by the parents of the patient.

Plants

Seed stocks: N/A

Novel plant genotypes: N/A

Authentication: N/A

Magnetic resonance imaging

Experimental design

Design type: Clinical exam acquired per standard clinical protocols

Design specifications: Clinical exam acquired per standard clinical protocols

Behavioral performance measures: N/A

Acquisition

Imaging type(s): Clinical exam acquired per standard clinical protocols

Field strength: 3T

Sequence & imaging parameters: Clinical exam acquired per standard clinical protocols

Area of acquisition: Clinical exam acquired per standard clinical protocols

Diffusion MRI ☒ Used ☐ Not used

Parameters: Clinical exam acquired per standard clinical protocols

Preprocessing

Preprocessing software: Clinical exam acquired per standard clinical protocols

Normalization: Clinical exam acquired per standard clinical protocols

Normalization template: Clinical exam acquired per standard clinical protocols

Noise and artifact removal: Clinical exam acquired per standard clinical protocols

Volume censoring: Clinical exam acquired per standard clinical protocols

Statistical modeling & inference

Model type and settings: No statistical models were used as MRI was a clinical exam acquired per standard clinical protocols

Effect(s) tested: No effects were tested as MRIs were obtained per standard clinical protocols for structural purposes

Specify type of analysis: ☐ Whole brain ☐ ROI-based ☐ Both

Statistic type for inference (See Eklund et al. 2016): No statistical models were used.

Correction: No statistical models were used.

Models & analysis

n/a	Involved in the study
☒	☐ Functional and/or effective connectivity
☒	☐ Graph analysis
☒	☐ Multivariate modeling or predictive analysis